gout, urate, and crystal deposition disease

MDPI

Conference Report

The 15th European Crystal Network (ECN) Workshop—2024 ECN Abstract Proceedings

Frédéric Lioté [1,2,*], Fernando Perez-Ruiz [3], Hang-Korng Ea [1], Tristan Pascart [4], Tony Merriman [5,6] and Alexander So [7]

1 Université Paris Cité, Inserm UMR 1132, Hôpital Lariboisière Paris, F-75010 Paris, France; hang-korng.ea@aphp.fr
2 Feel'Gout, Rheumatology Department, GH Paris Saint-Joseph, Institut Arthur Vernes, F-75006 Paris, France
3 Rheumatology Division, Cruces University Hospital, Vizcaya, Medicine Department, Medicine and Nursing School, University of the Basque Country, 48940 Biskay, Spain; fperezruiz@ehu.eus
4 Department of Rheumatology, Lille Catholic Hospitals, Saint-Philibert Hospital, University of Lille, F-59160 Lille, France; pascart.tristan@ghicl.net
5 Department of Microbiology, University of Otago, Dunedin 9016, New Zealand; tony.merriman@otago.ac.nz
6 Division of Clinical Immunology and Rheumatology, University of Alabama at Birmingham, Birmingham, AL 35294, USA
7 Service of Rheumatology, Department of Musculoskeletal Medicine, Lausanne University Hospital, University of Lausanne, 1005 Lausanne, Switzerland; alexanderso@outlook.com
* Correspondence: frederic.liote.pro@outlook.fr

Abstract: 15th Anniversary this year: the ECN workshop is set up in Paris, down town. Every year ECN workshop offers a unique opportunity for clinicians and researchers interested in crystals, inflammation, crystal-induced diseases including gout, to present their latest results and discuss novel concepts. Twenty nine out of 52 accepted abstracts are reported here.

Keywords: ECN; gout; interleukin-1; treat-to-target; CPPD; cardiovascular; SGLT2i; PPi; chondrocalcinosis

Citation: Lioté, F.; Perez-Ruiz, F.; Ea, H.-K.; Pascart, T.; Merriman, T.; So, A. The 15th European Crystal Network (ECN) Workshop—2024 ECN Abstract Proceedings. *Gout Urate Cryst. Depos. Dis.* **2024**, *2*, 275–314. https://doi.org/10.3390/gucdd2030021

Academic Editor: Flora Szeri

Received: 16 September 2024
Accepted: 17 September 2024
Published: 19 September 2024

1. Introduction

This year we had our usual 2-day face-to-face meeting with more than 100 colleagues, including dozens of young investigators, from all over the world. Attendees came from Europe, Canada, USA, Oceania and Asia (Figure 1). We had a different venue this year, thanks to the **Institut du Cerveau et du Muscle** (ICM) who provided a nice and comfortable auditorium.

Thanks to the Scientific Committee, we received a record 52 abstracts, from which 23 were selected for oral communications and 30 posters were presented in two sessions. Last year, with our partner US G-CAN group, we reported these abstracts in the second issue of the GUCDD [1], the G-CAN journal. Similarly, this year, only abstracts with permission from their first and/or senior authors are presented herein. All oral communications and lectures have been recorded and are available online with accreditation. Among 23 oral communications, the highest rated abstract was awarded the 2024 ECN Prize: Ms Anosha Moses, MSc, and PhD student, from the University of Twente, Enschede, Netherlands. She presented the first results of a randomized control trial (RCT) in gout: "Treat-to-Target in gout yields superior outcomes compared to a Treat to Avoid Symptoms approach (results from **Gout TrEatment Strategy** (GO TEST) **OVERTURE trial**)". The trial provides evidence that it is better to treat-to-target (T2T), meaning lowering the urate level below 6.0 mg/dL, than to treat the gout flare only to avoid symptoms (T2S). This is the first time such an RCT has been conducted to address this major issue. As the ECN Prize Winner, she will be invited next year to the 16th ECN Workshop.

Figure 1. Attendees of the 15th ECN workshop.

The 2024 program can be found at **ECN Workshop (https://www.european-crystal-network.com/programme)**.

- **Thursday** morning was devoted to four keynotes on IL-1β, the key cytokine in crystal-induced inflammation, with the first one given by Prof Charles Dinarello from Denver, CO, USA, who focused his talk on an oral NRLP3 inhibitor currently in development in gout but also in cancer, etc. Prof Mihai Netea (The Netherlands) discussed trained immunity for IL-1β regulation. Prof. Musa Mhlanga (The Netherlands) provided insights on non-coding RNA regulation of IL-1β. Finally, Luke O'Neill (Ireland) described two aspects of IL-1β with respect to innate immunity and immunometabolism.
- Thursday afternoon was as usual **"the Calcium day"** for calcium crystal-related diseases, namely in osteoarthritis, in CNS disease, and in X-linked hypophosphatemia/Hyp mice.
- Thursday afternoon was also devoted to monosodium urate- and calcium crystal-induced inflammation, with variations according to macrophage responses and to urate-mediated DNA methylation.
- The **"Calcium day"** continued on **Friday** morning with three topics of interest:
    - "Particulates and NLRP3 inflammasome activation" by Tony Merriman (United States), who addressed the question of air pollution in triggering gout flare.
    - Hang-Korng Ea (France) discussed "Fasting and crystal-induced inflammation", since low calorie intake can improve inflammation.
    - Finally, "PPi homeostasis and human diseases" was updated by Christophe Duranton (France).
- Prof. Claudio Borghi, a distinguished cardiologist from Italy, addressed the key-issue of gout and cardiovascular issues.
- On Friday, **"the Gout day"**, updates on cardiovascular issues were presented with specific interest in "Mortality in gout: epidemiology" by Matts Dehlin (Sweden) and a potential role for "SGLT2i and gout" by Hyon Choi (United States).
- The "Loch Ness monster" is still alive, prompting the question as to "Which crystals are within wall arteries?", which was addressed by a radiologist (Fabio Becce (Switzerland))
- Robert Terkeltaub (United States) nicely addressed "The gut in gout", given that the microbiota is part of the disease.

- Finally, Augustin Latourte (France) presented an overview on the IL-6 pathway in crystal-induced arthritis, namely chronic CPPD arthritis.

We are planning the next 16th ECN workshop, Paris, 6th and 7th March 2025, at the same venue; save the date and register for updates on the ECN Website to be sure to get information (https://www.european-crystal-network.com/).

2024 Scientific Committee: Prof. Nathalie Busso (SW), Prof. Dr Jessica Bertrand (GE), Dr Sonia Nasi (SW), Dr Tania Crisan (RO), Prof Michael Doherty (UK), Prof. Leo Joosten (NE), Prof. Robert Terkeltaub (US), Prof. Hyon Choi (US), Prof. Tony Merriman (US), Prof. Hang-Korng Ea (FR), Dr Hervé Kempf (FR), Prof. Tristan Pascart (FR), Prof. Alexander So (SW), Prof. Fernando Perez-Ruiz (SP), Prof. Frédéric Lioté (FR).

2024 Organizing Committee: Véronique Gordin (Médi-Evènement, FR), Prof Hang-Korng Ea (FR), Prof Fernando Perez-Ruiz (SP), Prof. Tristan Pascart (FR), Prof Frédéric Lioté (FR).

Thanks to our **2024 Sponsors**: AMGEN Rare Disease/Horizon Pharmaceuticals, Olatec, SOBI/Selecta.

Acknowledgments: Véronique Gordin, Médi-Evènement (FR) for organization and logistics, and Jean-Pierre Voisenet (FR) for technical and IT support.

2. Approach to the Association of Gout and Diabetes and Its Repercussions on Morbidity Using a Nationwide Dataset of Hospitalizations

Patricia Mora [1], Fernando Borrás [1], Eugenio De Miguel [2] and Mariano Andrés [1,3,4]

1 Miguel Hernandez University, 03550 San Juan de Alicante, Spain
2 La Paz Hospital, 28046 Madrid, Spain
3 Dr. Balmis General University Hospital-Isabial, 03010 Alicante, Spain
4 Alicante Institute for Health and Biomedical Research (ISABIAL), 03010 Alicante, Spain

Abstract: Introduction: Gout and diabetes mellitus (DM) are two highly prevalent diseases worldwide, closely related by pathophysiology. The implications of people with gout also presenting DM have received little attention in the literature, especially in terms of morbidity development. Objective: to analyze the impact of associating DM with gout in a nationwide hospitalized population in Spain. Methods: We analyzed the minimal basic dataset from 192,062 Spanish hospitalizations with gout (ICD-9 coding) from 2005 to 2015. The comorbidities of interest were cerebrovascular diseases, venous thromboembolism, sepsis, chronic kidney disease, arrhythmia, dementia, liver disease, obstructive pulmonary disease, and other rheumatic diseases, among others. Firstly, the prevalence of DM in the entire population was estimated, later stratified by type of DM (type 1 DM, type 2 DM, and other types of DM) and by whether it was complicated or not complicated, according to suitable ICD-9 codes, estimating their 95% confidence intervals (CI). We built a multiple logistic regression model to discern the characteristics of gouty patients with or without DM. Secondly, patients with repeated admissions in the dataset were identified and matched by age, sex, kidney disease, cardiovascular disease (combined from heart, cerebral, and peripheral disease), and infections (from pneumonia, urinary infections, and sepsis) within the first tertile (2005–2008). Later, we compared the frequencies of comorbidities of interest in the second (2009–2012) and third tertiles (2012–2015) using the chi-2 test. Results: In the gout dataset, the prevalence of DM was 27.7% (95% CI 27.5–27.9%). By subtypes, type 2 DM was far more prevalent (27.4%, 95% CI 27.2–27.6%) than type 1 (0.1%, 95% CI 0.1–0.2%) or other forms of DM (0.4%, 95% CI 0.3–0.4%). The presence of complicated DM was 19.8% (95% CI 19.4–20.1%) across all DM patients. Figure 2 shows the results of multiple logistic regression. Variables that most classified gouty people with DM were dyslipidemia, obesity, female sex, older age, and heart and renal diseases. On the other hand, venous thromboembolism and other concurrent rheumatic diseases were linked to those without DM.

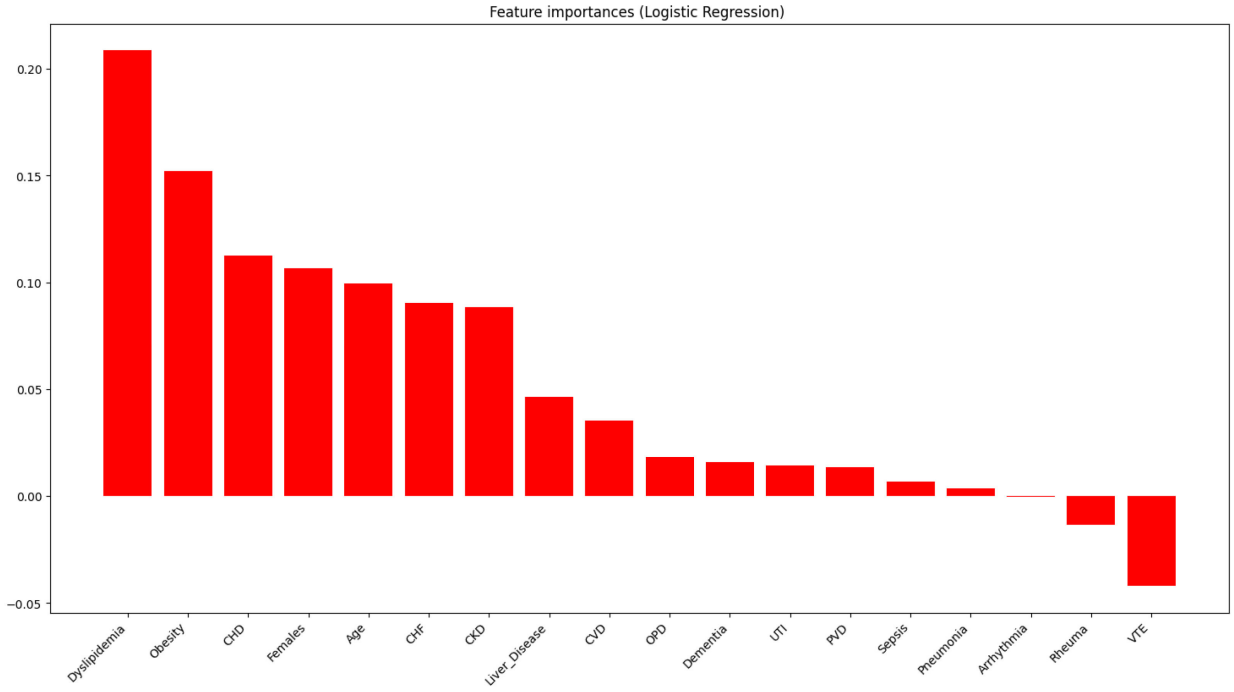

Figure 2. The results of multiple logistic regression.

Table 1 shows the distribution of comorbidities in patients with recurrent admission, finding increased numbers of ~10% for cardiovascular events (driven by coronary disease and heart failure) and kidney disease in those with DM, similar for infections and less presence of venous thromboembolism.

Table 1. The distribution of comorbidities in patients with recurrent admission.

	Tertile 1 (2005–2008)		**Tertile 2 (2009–2012)**		**Tertile 3 (2013–2015)**		
	No DM	**DM**	**No DM**	**DM**	**No DM**	**DM**	***p***
Cardiovascular disease	6169 (47.2)	6593 (48.8)	1033 (45.3)	934 (55.4)	388 (43.6)	354 (57.9)	<0.001
Cerebrovascular diseases	545 (4.2)	544 (4.0)	103 (4.5)	70 (4.1)	46 (5.2)	29 (4.7)	0.530
Coronary heart disease	3473 (26.6)	4029 (29.8)	565 (24.8)	505 (29.9)	193 (21.7)	200 (32.7)	<0.001
Congestive heart failure	2850 (21.8)	3077 (22.8)	534 (23.4)	522 (31.0)	187 (21.0)	200 (32.7)	<0.001
Peripheral vascular disease	500 (3.8)	522 (3.9)	86 (3.8)	68 (4.0)	43 (4.8)	27 (4.4)	0.709
Infections	1381 (10.6)	1415 (10.5)	283 (12.4)	199 (11.8)	123 (13.8)	81 (13.3)	<0.001
Pneumonia	515 (3.9)	524 (3.9)	94 (4.1)	83 (4.9)	45 (5.1)	31 (5.1)	0.119
Sepsis	94 (0.7)	89 (0.7)	40 (1.8)	22 (1.3)	19 (2.1)	12 (2.0)	<0.001
Urinary tract infection	832 (6.4)	855 (6.3)	170 (7.5)	107 (6.3)	68 (7.6)	43 (7.0)	0.238
Venous thromboembolism	347 (2.7)	262 (1.9)	46 (2.0)	27 (1.6)	31 (3.5)	14 (2.3)	<0.001
Chronic kidney disease	2427 (18.6)	2621 (19.4)	912 (40.0)	717 (42.5)	339 (38.1)	289 (47.3)	<0.001

Evolution of comorbidities of interest in patients with readmissions. Data are shown as *n* (%).

Conclusions: Analysis of 11 years of hospitalizations for gout confirms a different comorbidity profile between DM and non-DM, with a close relationship to metabolic syndrome. Assessing readmissions, the co-presence of DM had a significant impact on the cardiovascular and renal profiles of patients with gout, identifying no impact on infections and less risk of thromboembolism. Our findings may be interesting when treating a patient with gout and DM.

3. Safety and Efficacy of SEL-212 in Patients with Gout Refractory to Conventional Treatment: Outcomes from Two Randomized, Double-Blind, Placebo-Controlled, Multicenter Phase 3 Studies

Herbert S.B. Baraf [1,2], Alan Kivitz [3], Sheldon Leung [4], Olu Folarin [4], Joanna Sobierska [5], Jacquie Christie [5], Anand Patel [6], Wesley DeHaan [4], Rehan Azeem [4] and Peter Traber [4]

1 The Center for Rheumatology and Bone Research, Wheaton, MD 20902, USA
2 The George Washington University School of Medicine and Health Sciences, Washington, DC 20052, USA
3 Altoona Center for Clinical Research, Arthritis and Osteoporosis Center, Duncansville, PA 16635, USA
4 Sobi, Waltham, MA 02451, USA
5 Sobi, 4058 Basel, Switzerland
6 Conquest Research, Winter Park, FL 32789, USA

Abstract: Background: Sustained hyperuricemia may lead to severe clinical manifestations in gout refractory to conventional urate-lowering therapy (ULT). Uricase-based therapies can be effective, although immunogenicity can reduce efficacy. SEL-212 is a novel, once-monthly, two-component, uricase-based infusion therapy being investigated in patients with refractory gout. SEL-212 consists of sequential infusions of nanoparticles containing sirolimus (SEL-110), which provide tolerance to the subsequent infusion of pegadricase (SEL-037), a pegylated uricase. Objective: DISSOLVE I and II (D1 and D2, respectively) evaluated the safety and efficacy of SEL-212 in adults with refractory gout. Methods: D1 (US study, 12 months) and D2 (global study, 6 months), were placebo-controlled, double-blind, randomized clinical trials that evaluated two dose levels of SEL-110 (0.15 mg/kg (high-dose) or 0.1 mg/kg (low-dose)) prior to SEL-037 (0.2 mg/kg) infusion in adults (19–80 years). Participants with a history of symptomatic gout were enrolled if they had $\geq$3 gout flares within 18 months prior to screening or/and $\geq$1 tophus or a current diagnosis of gouty arthritis, had failed to normalize sUA and had inadequate control of signs and symptoms with medically appropriate doses of oral ULT, or had contraindications to such treatment and had not previously been exposed to a uricase-based therapy. Participants were randomized 1:1:1 between high- and low-dose SEL-212 and placebo administered intravenously every 28 days for 6 treatments. D1 participants were continued in a 6-month blinded extension phase under the initial treatment conditions. The primary endpoint was defined as the percentage of participants who achieved and maintained sUA < 6 mg/dL for $\geq$80% of the sixth 28-day treatment period (TP6) in the active treatment groups (response rate). Safety and tolerability were assessed through monitoring of adverse events (AEs) and laboratory testing. Results: A total of 265 participants (D1, n = 112 (96% male, 66% $\geq$50 years); D2, n = 153 (97% male, 72% $\geq$50 years) were randomized and dosed into the three treatment arms. Response rates in both active treatment groups were significantly greater versus placebo ($p \leq 0.0008$), with 56% and 46% of participants responding in the high-dose group and 48% and 40% in the low-dose group for D1 and D2, respectively. The response rates in participants aged $\geq$50 years were 65% and 47% in the high-dose groups and 47% and 44% in the low-dose groups for D1 and D2, respectively ($p \leq 0.0026$ vs. placebo). Across all participants in the treatment groups, median sUA levels were reduced by ~97% and ~66% from baseline at TP6 for D1 and D2, respectively. The safety profile of SEL-212 was favorable, with 3.4% and 4.5% of participants experiencing infusion reactions in the high- and low-dose groups, respectively. Reports of gout flares were comparable between treatment groups and placebo. Six participants (3.4%) in the pooled active treatment

groups experienced treatment-related serious AEs (n = 4 anaphylaxis, n = 2 gout flares). Conclusions: In the DISSOLVE trials, once-monthly treatment with SEL-212 demonstrated statistically significant response rates and reductions in sUA versus placebo. The safety profile of SEL-212 was consistent with that of uricase therapies. Targeted immunomodulation with SEL-212 has the potential to provide a new uricase-based treatment option for patients with gout refractory to conventional therapies without the need for traditional immunosuppressants.

Adaptation from: Baraf, H.S.B., Arthritis Rheumatol. 2023;75 (Suppl. 9): abstract number 0246.

Funding: The DISSOLVE I and II (NCT04513366 and NCT04596540) studies were jointly funded by Sobi and Selecta BioSciences, Inc., and this publication was funded by Sobi.

Author disclosures: Herbert S.B. Baraf—consultant: Sobi, Selecta BioSciences, Grünenthal and Olatec; speakers bureau: Horizon Pharmaceuticals; grant/research support from Horizon Pharmaceuticals, Sobi. Alan Kivitz—consultant: Janssen, AbbVie, Gilead, Grünenthal, Chemocentryx, Coval, Fresenius Kabi, Genzyme, GSK, Horizon, Prime, Prometheus, Selecta, Synact, Takeda-Nimbus, UCB, XBiotech, and ECOR1; speakers bureau: Eli Lilly, Flexion, AbbVie, Amgen, Sanofi—Regeneron, and GSK; shareholder of Pfizer, GSK, Gilead, Novartis, and Amgen. Anand Patel—speakers bureau: Lexicon Pharmaceuticals. Sheldon Leung is shareholder of Selecta Biosciences, and employee of Sobi. Olu Folarin—shareholder of Selecta Biosciences, employee of Sobi. Joanna Sobierska is employee of Sobi. Jacquie Christie is employee of. Sobi. Rehan Azeem is shareholder of: Selecta Biosciences and employee of Sobi. Wesley DeHaan is shareholder of Selecta Biosciences and employee of Sobi. Peter G. Traber is shareholder of Selecta Biosciences and employee of Sobi.

4. Urate-Induced Immunometabolic Adaptations of Myeloid Cells

Georgiana Cabău [1], Viola Kluck [2], Valentin Nica [1], Orsolya Gaal [1,2], Medeea Badii [1,2], HINT-consortium, Tania O. Crișan [1,†] and Leo A.B. Joosten [1,2,†]

[1] Department of Medical Genetics, "Iuliu Haţieganu" University of Medicine and Pharmacy, 400012 Cluj-Napoca, Romania
[2] Department of Internal Medicine, Radboud UMC, 6525 Nijmegen, The Netherlands
[†] Tania O. Crișan and Leo A.B. Joosten share senior authorship.

Abstract: Background: Hyperuricemia is the main risk factor for gout and is associated with a higher incidence of cardiometabolic disorders. Urate exposure in vivo alters the serum proteome towards higher inflammation, while in vitro studies reveal that soluble urate primes myeloid cells for higher induction of inflammatory cytokines by increasing IL-1beta production and reducing the anti-inflammatory cytokine, IL-1Ra. Moreover, the inflammatory memory induced by urate has been shown to modify the chromatin landscape, suggesting that epigenetic modifications could mediate the long-term detrimental effects of urate exposure. In the present study, we aim to unravel the underlying metabolic adaptations of urate-exposed myeloid cells. This will not only expand our understanding of the multifaceted nature of urate-induced inflammation but can potentially reveal new therapeutic targets aimed at preventing cardiometabolic complications associated with hyperuricemia. Methods: In a uric acid priming design, Percoll-enriched monocytes from healthy volunteers were treated with increasing concentrations of soluble uric acid in the absence or presence of pharmacological modulators 3PO, an inhibitor of the rate-limiting glycolysis enzyme PFKFB3, Acetyl-CoA, and the fatty acid synthase (FASN) inhibitor C75 for 24 h. After incubation, cells were washed and stimulated for another 24 h with LPS and monosodium urate crystals (MSU). Cytokine production was determined by ELISA. Transcriptomic data from in vitro soluble urate-stimulated PBMCs were assessed for differential expression of genes involved in the glycolytic and fatty acid synthesis pathways. Results: In vitro soluble urate exposure enhances proinflammatory cytokine production. Inhibition of glycolysis lowers the urate-induced inflammatory response. Addition of acetyl-CoA, the substrate for fatty acid synthesis on 3PO pre-treated myeloid cells, rescues the urate-induced proinflammatory phenotype. Inhibition of FASN the rate-limiting enzyme in the

FA synthesis pathway blocks uric acid priming, lowers proinflammatory cytokine production, and restores the anti-inflammatory IL-1Ra. Transcriptomic analysis corroborates these findings and reveals upregulation of the *PFKFB3* and *FASN* in urate-exposed PBMCs. Conclusions: Our preliminary data reveal that soluble urate rewires the metabolism of myeloid cells towards enhanced glycolysis and fatty acid synthesis. Cooperation of these two pathways converges to sustain the long-term inflammatory memory of urate exposed cells. Our data support a role of urate-induced metabolic adaptations and reveal new targetable pathways as a strategy for preventing hyperuricemia-induced inflammation.

5. Risk of Cardiovascular Events in Patients with Gout Starting Urate-Lowering Therapy with or without Flare Prophylaxis with Colchicine: An Emulated Target Trial Using English Primary Care, Hospitalisation, and Mortality Data

Edoardo Cipolletta, Georgina Nakafero, Anthony J. Avery, Mamas A. Mamas, Laila J. Tata, Abhishek Abhishek

Academic Rheumatology, University of Nottingham, Nottingham NG7 2RD, UK

Abstract: Background: Gout flares are associated with cardiovascular events (CVEs). Clinical trials show that low-dose colchicine reduces the risk of CVEs in patients with atherosclerotic cardiovascular diseases [1,2]. A recent study reported an increased risk of myocardial infarction (MI) in people with gout starting urate-lowering therapy (ULT) with colchicine [3]. Objective: to estimate the risk of CVEs among patients with gout initiating ULT with colchicine flare prophylaxis compared with no prophylaxis. Methods, study design, and population: English patients with a new diagnosis of gout starting ULT for the first time were included in a new-user cohort study using an emulated target trial design with propensity score overlap weighting. Exposure: colchicine prophylaxis vs. no prophylaxis. Patients co-prescribed colchicine for $\geq$21 days were compared with patients not prescribed colchicine or NSAIDs for $\geq$21 days on the same date as ULT initiation. Main outcome: first CVE (fatal and non-fatal stroke or MI) after cohort entry. Secondary outcomes: first-ever CVEs, fatal CVEs, MI, stroke. Negative control outcomes: respiratory tract infections, peptic ulcer disease. Positive control outcome: diarrhoea. Follow-up: We performed intention-to-treat (ITT) and per-protocol (PP) analyses. In ITT, follow-up was from ULT initiation to 180 days. In PP, follow-up was censored earlier if exposed patients ended prophylaxis, switched to NSAID prophylaxis, or if controls were prescribed prophylaxis. Statistical analysis. We used Cox proportional hazards models to obtain adjusted hazard ratios (aHR). We calculated adjusted incidence rates (aIR), adjusted risk differences (aRD), and E-values. In the PP analyses, an inverse probability of censoring weighting was applied. Results: 99,800 patients were included (Figure 3): mean (SD) age 62.8 (15.5) years, 25,511 (25.6%) female, 4063 (4.1%) with prior CVE, median (IQR) disease duration 0.2 years (0–2.4) and mean (SD) serum urate 516.4 micromol/L (94.1). Nearly all patients started allopurinol (99.3%). Controls and exposed patients were followed-up for 176.9 (26.7) and 175.5 (29.7) days in the ITT analysis and 161.1 (49.5) and 45.7 (33.1) days in the PP analysis. Patients with colchicine prophylaxis had lower risks of CVEs compared to those without prophylaxis in both the ITT (aHR: 0.82, 95% CI: 0.69–0.94) and PP analyses (aHR: 0.79, 95% CI: 0.58–0.99) (Table 2). There was no evidence of effect modification by age, gender, cardiovascular risk category, and year of ULT initiation in stratified analyses (not shown). Colchicine prophylaxis was not associated with negative control outcomes (not shown). The E-values (95% CI lower bound) for ITT and PP analyses were 1.74 (1.32) and 1.85 (1.11). Conclusions: Colchicine prophylaxis is associated with a reduced risk of CVEs when initiating ULT.

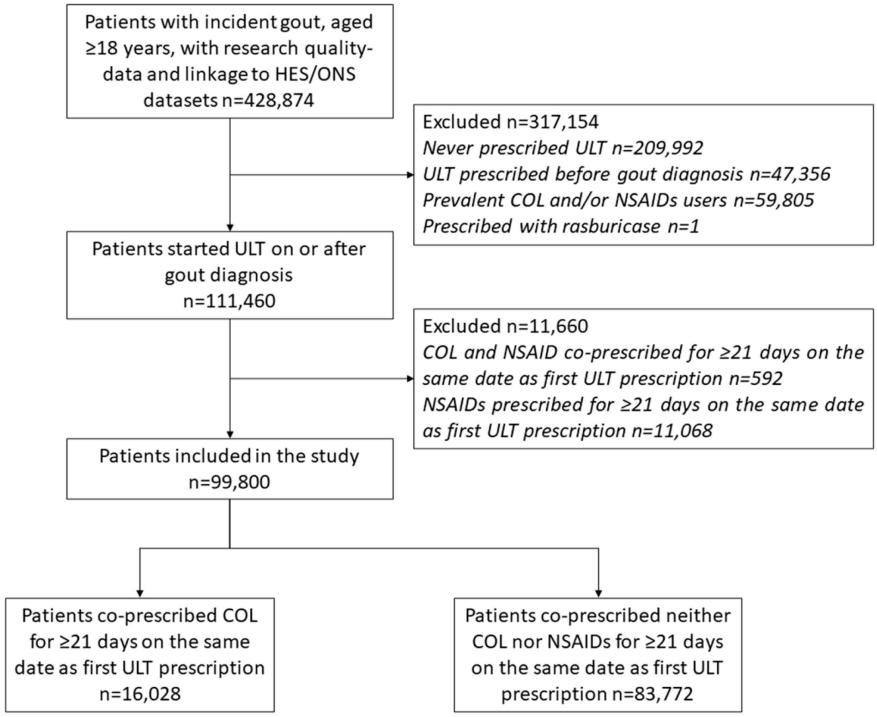

Figure 3. Flowchart of patient selection.

Table 2.

	Control Group (N = 83,772)			Colchicine Group (N = 16,028)			aHR	aRD (1000 Person Years)
	Events	Follow-Up Time (Person Years)	aIR (1000 Person Years)	Events	Follow-Up Time (Person Years)	aIR (1000 Person Years)		
ITT								
CVEs	1528	40,566.6	35.3 (33.0–37.9)	217	7700.4	28.8 (25.2–33.2)	0.82 (0.69–0.94)	−6.5 (−9.4 to −3.6)
First-ever CVEs	746	39,100.6	18.7 (17.0–20.7)	110	7465.1	14.8 (12.3–18.0)	0.80 (0.62–0.97)	−3.9 (−6.0 to −1.8)
Fatal CVEs	181	40,566.6	3.7 (3.0–4.7)	20	7700.4	2.7 (1.8–4.4)	0.74 (0.37–1.10)	−1.0 (−1.9 to −0.1)
MI	796	40,566.6	18.2 (16.5–20.0)	115	7700.4	15.1 (12.6–18.3)	0.84 (0.66–1.00)	−3.1 (−5.2 to −1.0)
Stroke	982	40,566.6	23.0 (21.1–25.0)	168	7700.4	22.1 (19.0–26.0)	0.94 (0.79–1.11)	−0.9 (−3.4 to 1.6)
PP								
CVEs	1416	36,948.3	39.7 (36.9–42.9)	69	2004.7	35.8 (29.1–42.4)	0.79 (0.58–0.99)	−3.9 (−7.1 to −0.7)
First-ever CVEs	690	35,595.4	20.7 (18.6–23.1)	29	1935.4	15.5 (10.8–21.1)	0.84 (0.50–1.17)	−5.2 (−7.3 to −3.1)
Fatal CVEs	167	36,948.3	4.3 (3.4–5.4)	9	2004.7	4.6 (2.4–10.2)	1.11 (0.34–1.88)	0.3 (−0.8 to 1.4)
MI	746	36,948.3	21.1 (19.0–23.4)	39	2004.7	20.2 (14.8–28.4)	0.83 (0.54–1.12)	−0.9 (−3.3 to 1.5)
Stroke	902	36,863.3	25.6 (23.3–28.3)	50	2001.0	24.8 (21.1–37.4)	0.90 (0.62–1.18)	−0.8 (−2.6 to 3.0)

References

1. Tardif, J.C.; Kouz, S.; Waters, D.D.; Bertrand, O.F.; Diaz, R.; Maggioni, A.P.; Pinto, F.J.; Ibrahim, R.; Gamra, H., Kiwan, G.S.; et al. Efficacy and Safety of Low-Dose Colchicine after Myocardial Infarction. *N. Engl. J. Med.* **2019**, *381*, 2497–2505.
2. Nidorf, S.M.; Fiolet, A.T.L.; Mosterd, A.; Eikelboom, J.W.; Schut, A.; Opstal, T.S.J.; The, S.H.K.; Xu, X.-F.; Ireland, M.A.; Lenderink, T.; et al. Colchicine in Patients with Chronic Coronary Disease. *N. Engl. J. Med.* **2020**, *383*, 1838–1847.
3. Roddy, E.; Bajpai, R.; Forrester, H.; Partington, R.J.; Mallen, C.D.; Clarson, L.E.; Padmanabhan, N.; Whittle, R.; Muller, S. Safety of colchicine and NSAID prophylaxis when initiating urate-lowering therapy for gout: propensity score-matched cohort studies in the UK Clinical Practice Research Datalink. *Ann. Rheum. Dis.* **2023**, *82*, 1618–1625.

6. Ionic Profile of Synovial Fluids in Gout, Calcium Pyrophosphate Crystal Deposition Disease, and Osteoarthritis

Mete Kayatekin [1,*], Dione Saurat [1], Isabelle Rubera [1], Charles Leroy [2], Pascal Richette [2,3], Hang-Korng Ea [2,3] and Christophe Duranton [1]

[1] Laboratoire de Physiomédecine Moléculaire, University Côte d'Azur, CNRS UMR-7370, Labex ICST, Nice, France
[2] Viggo Petersen Center, Bioscar, INSERM UMR-1132, Université Paris Cité, Hôpital Lariboisière, AP-HP, Paris, France
[3] Viggo Petersen Center, Rheumatology Department, DMU Locomoteur, Hôpital Lariboisière, AP-HP, Paris, France
* Correspondence: mete.kayatekin@etu.univ-cotedazur.fr

Abstract: Gout, secondary monosodium urate (MSU) crystal deposition, calcium pyrophosphate (CPP) crystal deposition (CPPD), and osteoarthritis (OA) are the main adult arthropathies responsible for joint swelling and pain. The analysis of synovial fluid (SF) is the key procedure in the diagnosis of these diseases. The SF of MSU and CPP crystal-induced joint inflammation is characterized by the presence of the pathogenic crystals and a high concentration of cells (>2000/mL). In contrast, OA SF contain a low cell concentration (<1500/mL). The SF cell concentration distinguishes the inflammatory and mechanical causes of arthropathies. However, our knowledge of synovial fluid ions' composition is very limited. The aims of this study were to characterize the composition and the ion concentrations of SF in gout, CPP crystal deposition, and OA. Methods: SF was harvested from patients who experienced joint swelling during gout flare (n = 19), CPP crystal-induced flare (n = 22) or OA (n = 33). SF was centrifuged and supernatants were collected and stored at −80 °C until analysis. SF osmotic pressure (OsP) was measured using the freezing point technique (Roebling Osmometer automatic) and concentration of the main ions (lactate, Cl^-, citrate, sulfate, phosphate and pyrophosphate (PPi)) by ion chromatography (Dionex, ICS-5000). Results: Our data (see Table 3 below) showed significant difference in osmotic pressure in the SF of patients diagnosed with OA compared to gout or CPPD. We also measured significant difference in the anionic profiles of the different SF samples; the lactate concentration was higher in SFs of CPPD and in gout patients compared to OA. Chloride and citrate concentrations were significantly lower in gout and CPPD patients compared to OA. Moreover, we did not see any difference in sulfate and phosphate concentration. Interestingly, in SFs from gout patients, we measured a significantly lower PPi concentration compared to OA or CPPD.

For the first time in a large cohort of 74 patients, the ion concentrations and osmotic pressure of SFs harboring different arthropathies were measured. According to our results, we observed a specific ion concentration profile in crystal-mediated arthropathies (lower osmotic pressure and chloride concentration and higher lactate concentration) compared to OA. Additionally, we also measured a lower PPi concentration in gout SFs compared to OA or CCA diseases, suggesting that PPi might be considered a valuable biomarker for

differentiating between different arthropathies. Altogether, our results suggest that SF is a dynamic fluid and ion concentrations vary between the different arthropathies.

Table 3. Difference in osmotic pressure in SF of patients diagnosed with OA compared to gout or CPPD.

	Gout (MSU)	(CPPD) Disease	Osteoarthritis (OA)
OsP (mOsml/L)	288 ± 5	283 ± 6	319 ± 8
Lactate (mM)	5.06 ± 0.57	5.75 ± 0.51	3.3 ± 0.16
Chloride (mM)	125 ± 3	114 ± 3	131 ± 4
Citrate (μM)	116 ± 15	140 ± 38	176 ± 14
Sulfate (μM)	400 ± 47	324 ± 41	312 ± 16
Phosphate (mM)	0.32 ± 0.07	0.56 ± 0.1	0.53 ± 0.09
PPi (μM)	1.9 ± 0.4	5.2 ± 1.3	6.9 ± 0.9

7. Differences in the Inflammatory Proteome of Gout Patients during Flare, Inter-Critical and T2T Conditions Reveal New Disease Biomarkers

Brenda Kischkel [1,*], Twinu Wilson Chirayath [2], Tim L. Jansen [3], Mylène Zarka [2], Tania Criçan [4], Mihai G Netea [1], Pascal Richette [2], Leo A. B. Joosten [1,4] and Hang-Korng Ea [2]

1 Department of Internal Medicine, Radboud University Medical Center, 6500HB, Geert Grooteplein Zuid 10, 6525 Nijmegen, The Netherlands
2 Université de Paris, Hôpital Lariboisière, INSERM UMR 1132, AP-HP, 75457 Paris, France
3 VieCuri Medical Centre, Department of Rheumatology, Complex Gout Expert Centre, Venlo, The Netherlands
4 Department of Medical Genetics, Iuliu Hatieganu University of Medicine and Pharmacy, 400012 Cluj-Napoca, Romania
* Correspondence: brenda.kischkel@radboudumc.nl

Abstract: Background: Gout flares are characterized by severe attacks of pain, swelling, redness, and tenderness that can last for 7 to 10 days, followed by an inter-critical period, which is an asymptomatic stage between flares. To prevent relapses of gout flares, urate-lowering therapy (ULT) is used and can be linked to a treat-to-target (T2T) approach, in which the medication doses are adjusted until serum urate concentrations are below 0.36 mmol/L. Objectives: In this study, we accessed the plasma proteomic profile of patients included in a prospective study (GOUTROS cohort) in order to characterize the systemic inflammatory profile of gout patients during flare (T1), inter-critical (T2), and T2T (T3) conditions. Methods: Proximity extension assay technology (Olink) was used to measure 92 inflammation-related molecules in 71 enrolled patients. Our findings were validated in an independent cohort of patients, followed by in vitro and in vivo experiments to understand the involvement of a new biomarker in the context of gout flares. Findings: We identified 19 proteins (26.8%) that were differentially expressed (FDR < 0.05) between T1 (Flare) and T2 (inter-critical) and 13 proteins (18.3%) between T1 and T3 (T2T). Among them, IL-6, TNFSF14, CSF-1 and VEGFA were highly expressed during T1. TRANCE and Flt3L increased significantly during T2 and T3, respectively, when compared with T1. Of interest, IL-6 expression was correlated to the presence of tophi, in which patients with high levels of IL-6 during the inter-critical period presented tophi (p = 0.002, AUC 0.7). Next, we performed the same proteomic analysis on an independent cohort of patients to validate the expression of biomarkers observed during a gout flare. TNFSF14 and IL-6 were the most significantly expressed during flare in both cohorts. While the role of IL-6 in MSU crystal-induced inflammation is well known, the role of TNFSF14 has not been described before. Thus, we investigated its contribution in crystal-induced inflammation. To achieve this goal, we exposed human PBMCs to a TNFSF14 inhibitor as well as the

recombinant TNFSF14 protein followed by stimulation with MSU crystals and LPS. We observed that the production of proinflammatory cytokines, such as IL-6, TNF and IL-1β, significantly decreased in the presence of the inhibitor and increased in the presence of the recombinant protein. Of clinical importance, we were able to detect TNFSF14 being produced locally in the synovial fluid of patients with gout and in air pouch membranes of mice injected with MSU crystals. Finally, using a cohort of 164 healthy individuals from the human functional genomics project (HFGP, 200FG), we demonstrated that PBMCs from individuals carrying variants of the *TNFSF14* gene showed production of inflammatory cytokines that was affected in response to MSU crystals and LPS. Individuals carrying rs344559 exhibited decreased production of IL-1β, while individuals carrying rs2101765 showed increased production of IL-1β and IL-6. Significance: This study will help to improve our understanding of how the human immune system reacts in different stages of gout, allowing the identification of TNFSF14 as a new biomarker associated with gout flares. Collectively, our results also suggest that TNFSF14 could modulate the inflammatory response during a gout flare and may be considered a therapeutic target.

8. Gout Remission: Perceptions of Rheumatologist, Nephrologist, and Primary Care Physicians

Yael Klionsky [1], Eunice Luo [2], Sara Vazquez Irizarry [3], Lissa Padnick-Silver [2], Brian LaMoreaux [2] and Gordon Lam [4]

1 Wake Forest University School of Medicine, Winston-Salem, NC 27101, USA
2 Amgen Inc., Deerfield, IL 60015, USA
3 Buzzback LLC, New York, NY 10018, USA
4 Arthritis & Osteoporosis Consultants of the Carolinas, Charlotte, NC 28207, USA

Abstract: Background: Gout is associated with increased comorbidity [1] and cardiac and all-cause mortality [2,3,4] and lower quality of life (QOL) [5], suggesting systemic consequences of this inflammatory arthritis. Patients who have high serum urate levels (SU) with ongoing gout signs/symptoms (flares, non-resolving tophi) despite maximum tolerated xanthine oxidase inhibitor dosing (uncontrolled/refractory gout) have even worse health and QOL scores [6,7]. As a result, the goal of treating gout to remission has emerged as an important clinical target. However, a clear definition of gout remission has yet to be determined. Therefore, understanding how physicians define and view gout remission is of increasing importance, particularly with growing evidence of systemic consequences of local gout flares. Methods: Board-certified rheumatologists, nephrologists, and primary care physicians (PCPs) who were registered in the Physician Insights Platform (Sermo, New York, NY) were invited to participate. An online questionnaire was completed in July 2023 by interested physicians who were experienced practitioners (2–35 years in practice), spent most of their time ($\geq$75%) on patient care, saw $\geq$150 patients in the prior month, and managed $\geq$10 gout patients in the prior month. Clinical criteria, timing, and feasibility of gout remission were examined and compared between physician types. Returned surveys were excluded from analyses if data were of poor quality (completion time too long/short, poor open-ended responses, all items responded to with the same answer). Data collection, validation, and preliminary analysis were performed by buzzback LLC (New York, NY, USA). Results: A total of 363 surveys were completed, of which 10 were excluded from analyses because of poor open-ended responses. Therefore, data from 353 physicians were included, with nearly all (90%) reporting familiarity and comfort with treating gout to remission. Rheumatologists (n = 151) and nephrologists (n = 100) viewed gout remission as SU control with the absence of flares and gout-related pain (includes tender or swollen joints). In contrast, PCPs (n = 102) did not include SU control, relying mainly on general symptom control (absence of gout flare and gout-related pain, top of Figure 4). Most physicians agreed that for patients to have gout remission, these criteria needed to be met for 6–12 months. The top potential hinderances for treating gout to remission were viewed most often as medication non-adherence (83%), high monosodium urate (MSU) crystal burden (76%), patient lifestyle non-compliance (75%), and patient comorbidities (74%; score

of 1–2 on a 7–point scale). Patient lifestyle was rated as a top hinderance for remission more often by PCPs (83%) than rheumatologists (72%) and nephrologists (70%). MSU crystal burden was rated as a top hinderance less often by PCPs (59%) than rheumatologists (85%) and nephrologists (79%; Figure 4, Bottom). Conclusions: Despite lack of a standardized definition of gout remission, treating physicians feel comfortable treating gout and including remission as a goal. Differing from rheumatologists, a large proportion of PCPs and nephrologists did not report SU control as an important component of gout remission, relying more heavily on symptoms (gout flare, pain, disability). These differences may stem from differences in training, interest, experience, and gout management guidelines between the specialist [8,9] and primary care [10] communities. the findings of the current study highlight the need for and importance of a standardized definition of gout remission that includes SU control. Widespread adoption of this definition could help standardize gout care while emphasizing the importance of SU control to the primary care community, often the first line of contact and management for gout patients.

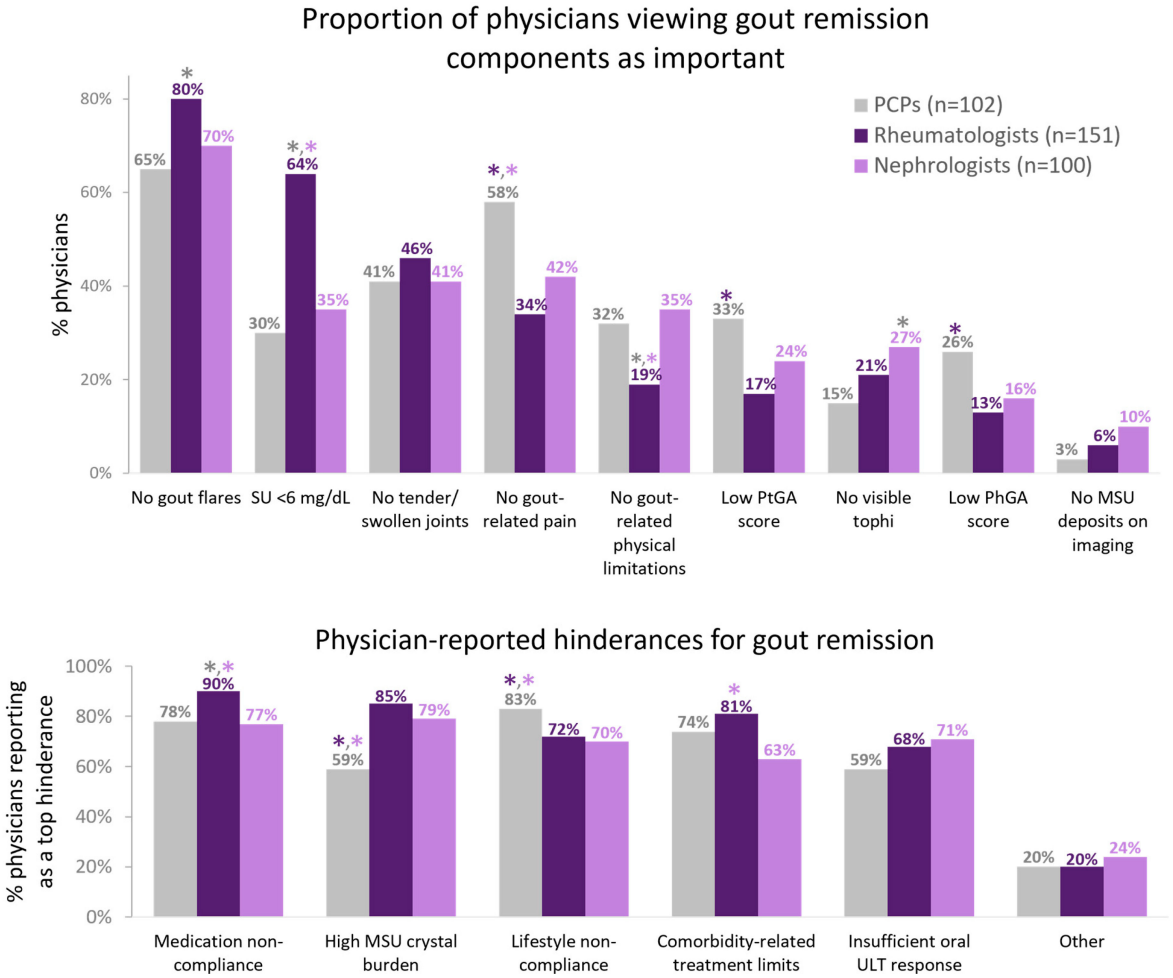

Figure. Top: Proportion of physicians ranking each gout remission criterion in their top 3 of importance (each item scored on a 7-point scale). **Bottom:** Proportion of physicians ranking potential hinderances of achieving gout remission in the top 2 of importance (each item scored on a 7-point scale). "Other" most-commonly included cost/insurance and medication side effects/intolerance. *significant difference from PCPs, *significant difference from rheumatologists, *significant difference from nephrologists ($p<0.05$). PCPs, primary care physicians; SU, serum urate; PtGA, Patient Global Assessment of Gout; PhGA, Physician Global Assessment of Gout; MSU, monosodium urate.

Figure 4. Top: Proportion of physicians ranking each gout remission criterion in their top three most important (each item scored on a 7-point scale). **Bottom**: Proportion of physicians ranking potential hinderances of achieving gout remission in the top two most important (each item scored on a 7-point scale).

References

1. Zhu, Y.; Pandya, B.J.; Choi, H.K. Comorbidities of gout and hyperuricemia in the US general population: NHANES 2007–2008. *Am. J. Med.* **2012**, *125*, 679–687.
2. Choi, H.K.; Curhan, G. Independent Impact of Gout on Mortality and Risk for Coronary Heart Disease. *Circulation* **2007**, *116*, 894–900.
3. Pérez Ruiz, F.; Richette, P.; Stack, A.G.; Karra Gurunath, R.; García de Yébenes, M.J.; Carmona, L. Failure to reach uric acid target of <0.36 mmol/L in hyperuricaemia of gout is associated with elevated total and cardiovascular mortality. *RMD Open* **2019**, *5*, e001015.
4. Kuo, C.F.; See, L.C.; Luo, S.F.; Ko, Y.S.; Lin, Y.S.; Hwang, J.S.; Lin, C.M.; Chen, H.W.; Yu, K.H. Gout: an independent risk factor for all-cause and cardiovascular mortality. *Rheumatology (Oxford)* **2010**, *49*, 141–146.
5. Singh, J.A.; Taylor, W.J.; Simon, L.S.; Khanna, P.P.; Stamp, L.K.; McQueen, F.M.; Neogi, T.; Gaffo, A.L.; Becker, M.A.; MacDonald, P.A.; et al. Patient-reported outcomes in chronic gout: a report from OMERACT 10. *J. Rheumatol.* **2011**, *38*, 1452–1457.
6. Francis-Sedlak, M.; LaMoreaux, B.; Padnick-Silver, L.; Holt, R.J.; Bello, A.E. Characteristics, Comorbidities, and Potential Consequences of Uncontrolled Gout: An Insurance-Claims Database Study. *Rheumatol. Ther.* **2021**, *8*, 183–197.
7. Khanna, P.P.; Nuki, G.; Bardin, T.; Tausche, A.K.; Forsythe, A.; Goren, A.; Vietri, J.; Khanna, D. Tophi and frequent gout flares are associated with impairments to quality of life, productivity, and increased healthcare resource use: Results from a cross-sectional survey. *Health Qual. Life Outcomes* **2012**, *10*, 117.
8. FitzGerald, J.D.; Dalbeth, N.; Mikuls, T.; Brignardello-Petersen, R.; Guyatt, G.; Abeles, A.M.; Gelber, A.C.; Harrold, L.R.; Khanna, D.; King, C.; et al. 2020 American College of Rheumatology Guideline for the Management of Gout. *Arthritis Care Res.* **2020**, *72*, 744–760.
9. Richette, P.; Doherty, M.; Pascual, E.; Barskova, V.; Becce, F.; Castañeda-Sanabria, J.; Coyfish, M.; Guillo, S.; Jansen, T.L.; Janssens, H.; et al. 2016 updated EULAR evidence-based recommendations for the management of gout. *Ann. Rheum. Dis.* **2017**, *76*, 29–42.
10. Qaseem, A.; Harris, R.P.; Forciea, M.A.; Clinical Guidelines Committee of the American College of Physicians; Denberg, T.D.; Barry, M.J.; Boyd, C.; Chow, R.D.; Humphrey, L.L.; Kansagara, D.; et al. Management of Acute and Recurrent Gout: A Clinical Practice Guideline From the American College of Physicians. *Ann. Intern. Med.* **2017**, *166*, 58–68.

Disclosures: Y. Klionsky has received consultancy fees from and/or served on advisory boards for MedIQ, Amgen, AstraZeneca, and Lilly. E. Luo, L. Padnick-Silver, and B. LaMoreaux are employees of and stockholders in Amgen. *S. Vazquez Irizarry is an employee of buzzback, who received funds from Amgen for survey administration and data collation. G. Lam received speaking and consulting honoraria from Amgen* (*formerly Horizon Therapeutics).

9. Prediagnostic Proteomics of Gout: Prospective Cohort Study of 48,898 Men and Women

Natalie Mccormick, Amit Joshi, Robert Terkeltaub, Tony R. Merriman, Chio Yokose, Hyon K. Choi

Massachusetts General Hospital and Harvard Medical School, Boston, MA 02115, USA

Abstract: Background: Detailed characterization of the plasma proteome may provide insights into the dynamic molecular changes preceding gout. A previous cross-sectional study of pre-existing gout (n = 7 candidate proteins) reported higher CXCL8 levels among prevalent gout vs. non-gout [1], but data on pre-diagnostic proteomic biomarkers are sparse. Objectives: We investigated the relation between large-scale pre-diagnostic proteomics and risk of incident gout in a nationwide prospective cohort, accounting for serum

urate levels, and explored biological mechanisms connected to the gout-associated proteins and upstream factors. Methods: We included 48,898 UK Biobank participants with proteomic measures and no history of gout or urate-lowering therapy use at baseline (2006–2010; mean age 56.7 years, 45% males). Proteomic measures (n = 2923, via Olink Explore 3072) were quantified from baseline blood samples via Olink's Proximity Extension Assay technology [2]. Eight proteins with >20% missingness were excluded. Multivariable Cox proportional hazards models were used to assess the association between protein levels and risk of incident gout (from linked primary care and inpatient diagnoses), before and after serum urate adjustment, using a false discovery rate (P_{FDR}) of <0.05. We performed two-sample Mendelian randomization (MR) to explore potential causal roles of the statistically significant proteins, leveraging genetic association data for loci mapping within 1 Mb of the protein-encoding gene controlling expression in *cis* [2], and from the GlobalGout GWAS [3]. We also used Ingenuity Pathway Analysis (IPA) software to explore the canonical pathways and upstream regulators enriched for the gout-associated proteins. Results: 1095 incident gout cases were documented over a mean follow-up period of 13.2 years. The levels of 1027 proteins were associated with risk of incident gout before urate adjustment (Figure 5), with the five strongest associations being with insulin-like growth factor-binding protein 4 (hazard ratio (HR) 1.60, 95% CI 1.51–1.69 per SD; P_{FDR} 2.5×10^{-57}), TNF receptor superfamily member 12A (1.53, 1.45–1.62; P_{FDR} 2.4×10^{-49}), N-acetylneuraminate lyase (1.52, 1.44–1.60; P_{FDR} 1.5×10^{-47}), uromodulin (0.67, 0.64–0.71; P_{FDR} 2.4×10^{-44}), and CD59 (1.42, 1.35–1.49; P_{FDR} 2.4×10^{-44}). Other key associations were CD38, a proinflammatory NAD-hydrolyzing enzyme expressed in macrophages; CCL16, a substantial monocyte chemoattractant; and ADM, which regulates inflammation bidirectionally, including in the synovium (Figure 5). A total of 41 proteins remained associated with risk of incident gout after serum urate adjustment, including uromodulin, as well as regenerating islet-derived protein 4, N-terminal prohormone of brain natriuretic peptide, sarcoplasmic reticulum histidine-rich calcium-binding protein, MAM domain-containing protein 2, and Spondin-1 (SPON1). MR findings supported causal roles that were directionally consistent for 72 of the 817 measurable proteins associated with gout before urate adjustment and 3 of 37 measurable proteins after urate adjustment (Secretagogin, SPON1, and TNF receptor superfamily member 6B). Figure 6 is an overview of the most significant upstream regulators and biological functions predicted in the IPA core analysis. The top biological pathways were pathogen-induced cytokine storm signalling ($P_{FDR} = 3.2 \times 10^{-48}$), hepatic fibrosis ($P_{FDR} = 1.3 \times 10^{-47}$), and neutrophil degranulation ($P_{FDR} = 1.3 \times 10^{-45}$). Pathways involved in wound healing signalling, regulation of insulin-like growth factor transport and uptake, and granulocyte adhesion and diapedesis were also among the top overrepresented biological pathways. TNF, a cytokine master regulator of inflammatory signaling, was identified as the top upstream regulator of gout-associated proteins. Other upstream regulators included transforming growth factor beta 1 (TGFB1) and IL-1B and IL-4 cytokines. Conclusions: These prospective findings provide insights into the pathophysiological mechanisms leading to gout, including after hyperuricaemia, and prioritize protein–gout genetic associations for future research.

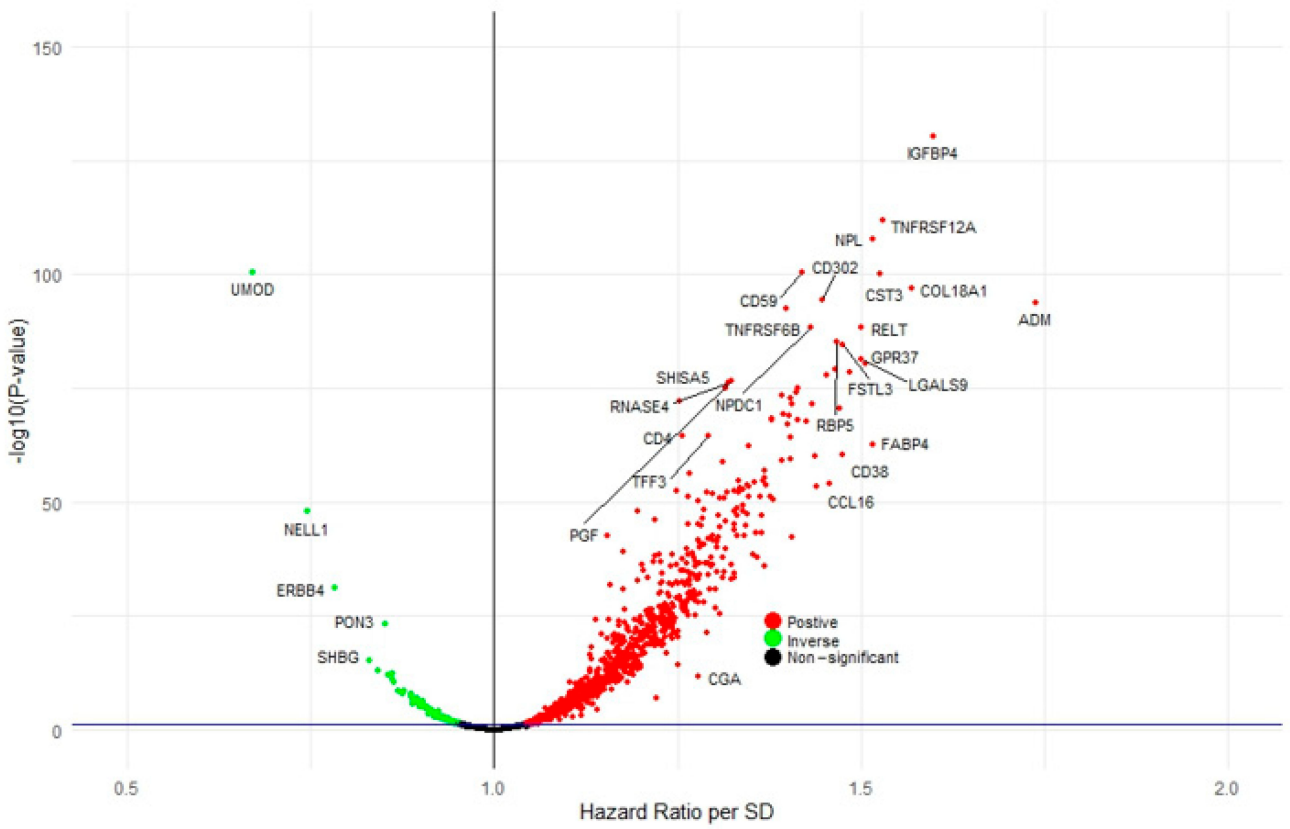

Figure 5. Volcano plot illustration the association of each of the 2915 candidate proteins with incident gout; selected proteins are labelled. Hazard ratio per standard deviation (SD) change in protein level generated from the multivariable Cox proportional hazards model, before serum urate adjustment, using a false discovery rate (P_{FDR}) of <0.05 (solid blue horizontal line).

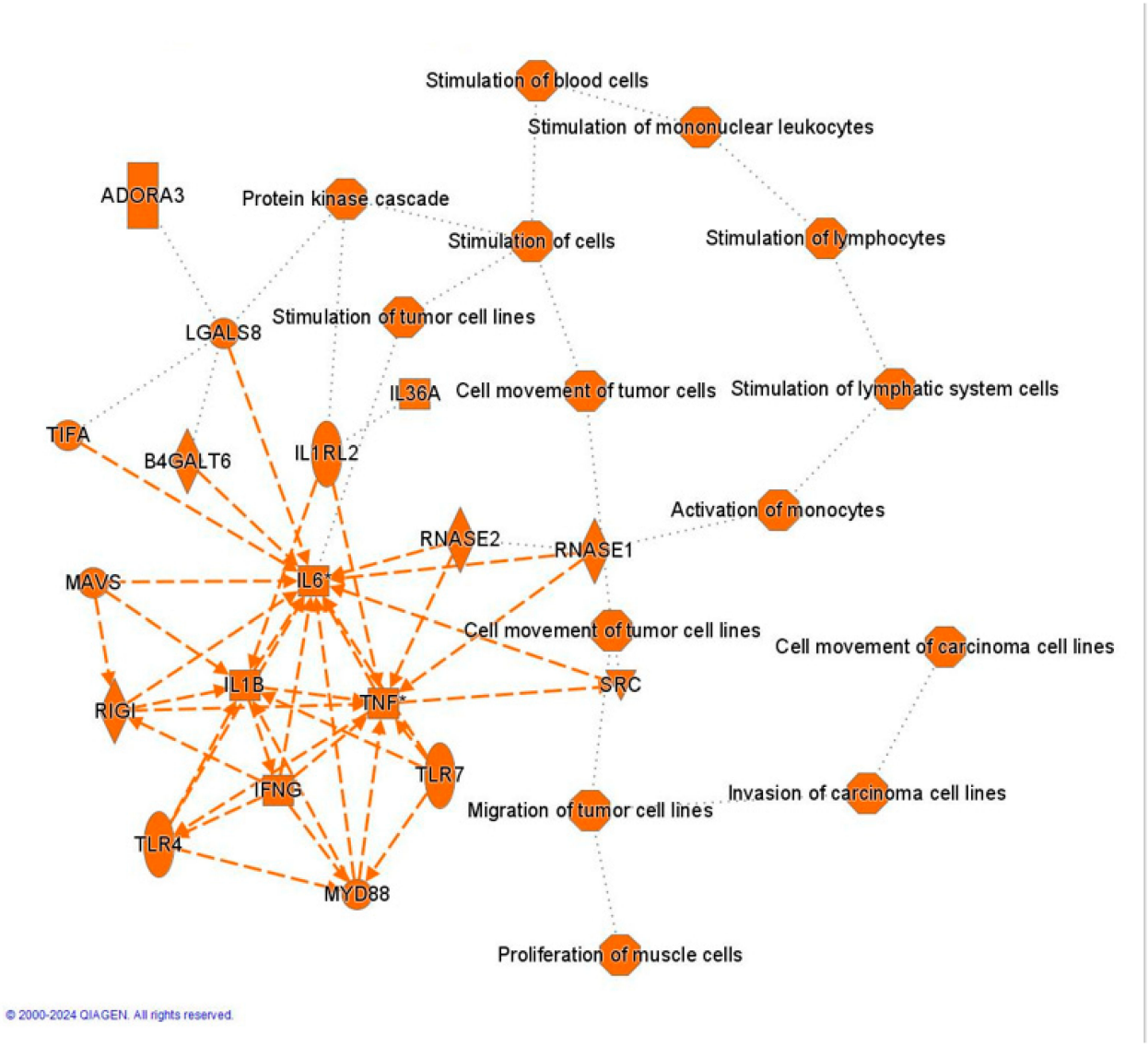

Figure 6. A graphical summary of the most significant upstream regulators, diseases, and biological functions predicted within the IPA core analysis based on the association between candidate proteins and incident gout risk. Orange lines indicate direct activation, whilst black dotted lines indicate inferred relationships. Squares indicate cytokines, ovals indicate transmembrane proteins, diamonds indicate enzymes, rectangles indicate G-protein coupled receptors, octagons indicate biological functions, and circles indicate proteins with other functions.

References

1. Mccormick, N.; Joshi, A.; Terkeltaub, R.; Merriman, T.; Yokose, C.; Choi, H. OP0051 prediagnostic proteomics of gout: prospective cohort study of 48,898 men and women. *Ann. Rheum. Dis.* **2024**, *83*, 4.
2. Sun, B.B.; Chiou, J.; Traylor, M.; Benner, C.; Hsu, Y.H.; Richardson, T.G.; Surendran, P.; Mahajan, A.; Robins, C.; Vasquez-Grinnell, S.G.; et al. Plasma proteomic associations with genetics and health in the UK Biobank. *Nature* **2023**, *622*, 329–338.
3. Major, T.J.; Takei, R.; Matsuo, H.; Leask, M.P.; Topless, R.K.; Shirai, Y.; Li, Z.; Ji, A.; Cadzow, M.J.; Sumpter, N.A.; et al. A genome-wide association analysis of 2,622,830 individuals reveals new pathogenic pathways in gout. *medRxiv* **2022**. https://doi.org/10.1101/2022.11.26.22281768.

10. Runt-Related Transcription Factor (RUNX) 1 Activation by Monosodium Urate Crystals Influences the Production of Inflammatory Cytokines in Human Monocytes

Laura M. Merlo Pich [1], Viola Klück [1], Liesbeth van Emst [1], Ruiqi Liu [1], Martin Jaeger [1], Tania Crisan [2], Mihai G. Netea [1,3], Yang Li [1,4] and Leo A.B. Joosten [1,2]

1 Department of Internal Medicine, Radboud University Medical Center, 6525 GA Nijmegen, The Netherlands
2 Department of Medical Genetics, Iuliu Hatieganu University of Medicine and Pharmacy, 400012 Cluj-Napoca, Romania
3 Department for Immunology and Metabolism, Life and Medical Sciences Institute (LIMES), University of Bonn, 53115 Bonn, Germany
4 Department of Computational Biology of Individualised Medicine, Centre for Individualised Infection Medicine (CiiM), a Joint Venture Between the Hannover Medical School (MHH) and the Helmholtz Centre for Infection Research (HZI), 30625 Hannover, Germany

Abstract: Background: Gout is one of the most common forms of inflammatory arthritis worldwide. Among the risk factors for gout, chronic hyperuricemia is the most relevant one. Nonetheless, a minority of people experiencing hyperuricemia will develop MSU crystals in the joints and symptomatic gout flares. This suggests that other factors may induce a predisposition to gout, including variations in the immune responses and their inflammatory pathways. These variations are to date not completely understood. Therefore, the aim of this study is to assess the genetic variations in human primary myeloid cells highlighted by a change in inflammatory cytokine production induced by acute stimulation with MSU crystals and to further explore the role of RUNX1 in these cells. Methods: PBMCs obtained from two cohorts of healthy volunteers were stimulated for 24 h with palmitic acid (C16.0) and monosodium urate (MSU) crystals. The obtained supernatants were used to measure cytokine production with ELISA assays (R&D). The same volunteers were also genotyped using the Illumina Human OmniExpress Exome-8 v1.0 SNP chip. A meta-analysis of genome-wide cQTL mapping in each cohort was performed. Next, we associated all annotated RUNX1 SNPs with cQTL data form the largest cohort. For in vitro validation, RUNX1 expression in PBMCs and U937 cells was assessed by qPCR and, to assess functional consequences, a RUNX1 knockdown cell line was generated and a RUNX1 inhibitor was tested on healthy donor PBMC. Results: rs4817731, 500 kb upstream of RUNX1, was identified as the top SNP associated with IL-6 production after C16.0 and MSU crystal stimulation (meta p-value $p = 1.37 \times 10^{-6}$). A total of 618 other SNPs annotated to RUNX1 also influenced either IL-1β or IL-6 release after stimulation ($p < 0.05$). Transcription of RUNX1 is upregulated in human PBMCs by stimulation with TLR ligand and/or MSU crystals or recombinant human IL-1β. RUNX1 knockdown in a monocytic cell line resulted in a reduction of cytokine production after stimulation with MSU and toll-like receptor agonists. Discussion. cQTL analysis revealed that RUNX1 could play a relevant role in MSU crystal-induced cytokine production and potentially in gout. This was supported by our in vitro experiments in which RUNX1 acts as a positive feedback loop for IL-1β. Further studies are warranted to assess the relevance of RUNX1 in gout in vivo and the prevalence among gout patients of the identified variation.

11. Treat-to-Target in Gout Yields Superior Outcomes Compared to a Treat-to-Avoid Symptoms Approach (Results from Gout TrEatment Strategy (GO TEST) OVERTURE Trial) (2024 ECN Prize)

Anusha Moses [1], Martijn Oude Voshaar [1,2], Tim Jansen [3] and Mart Van de Laar [4]

1 Medical Cell BioPhysics &TechMed Center, Department of Personalized Diagnostics and Therapeutics, University of Twente, 7522 Enschede, The Netherlands
2 Erasmus Medical Center, Department of Public Health, 3015 Rotterdam, The Netherlands
3 Viecuri Medical Center, Department of Rheumatology, 5912 Venlo, The Netherlands
4 Department of Psychology, University of Twente, 7522 Enschede, The Netherlands

Abstract: Background: Both the European League Against Rheumatism (EULAR) and the American College for Rheumatology (ACR) state that gout can be effectively managed by reducing sUA levels below the physiological threshold of saturation using urate-lowering therapy (ULT), a treat-to-target approach (T2T). An alternative, more reactive management strategy, advocated by the American College of Physicians (ACP), is to treat symptoms and to base the start and dosing of ULT on avoiding (recurrent) symptoms, without monitoring sUA levels. This treat-to-avoid symptom (T2S) approach has been criticized by rheumatologists for potentially ignoring ongoing urate deposition until potentially severe disease manifestations become apparent. Although the solid underlying mechanism of gout is ignored, the lack of a head-to-head comparison of both strategies led the ACP to advise the T2S strategy for the treatment of gout. Objectives: The objective of the Gout TrEatment Strategy (GO TEST) OVERTURE trial is to compare a T2T strategy versus a T2S strategy for the management of gout. Methods: The GO TEST OVERTURE study is a multicenter randomised controlled open-label pragmatic trial. Patients with a clinical diagnosis of gout, fulfilling the 2015 ACR-EULAR criteria, currently not using ULT but with an indication for the use of ULT were included. Patients with a contraindication for allopurinol, benzbromarone, and febuxostat, including those with an eGFR < 30 mL/min, were excluded from the study. Patients in the T2T group started ULT at the discretion of the attending physician. Their sUA levels were regularly measured and ULT dosages were titrated to achieve an sUA target of <0.36 mmol/L. In the T2S group, patients were instructed to self-monitor their gout symptoms and to contact the clinic in case of recurrent symptoms, with a potential ULT dosage increase in case of flare recurrence. The incidence of patient-reported gout flares was assessed every three months using the Gaffo gout flare criteria. The major outcomes of the study were the proportions of patients meeting the sUA target and the number of Gaffo flares during 1-year follow-up. The proportions of patients achieving the sUA target level were compared using z-tests for proportions. The number of flares over 1 year was compared using Poisson regression analysis. Results: A total of 308 patients were eligible and included in the trial (T2T n = 145; T2S n = 163) with a mean sUA of 0.5 and 0.4 mMol/L and mean age of 62.5 at baseline in each group, respectively. After 1 year, the proportion of patients achieving the target sUA level <0.36 mmol/L s was significantly higher in the T2T group (77%) than in the T2S group (29%) ($p < 0.001$). In addition, the incidence rate ratio for gout flares was 1.541 for T2S versus T2T ($p < 0.001$), indicating that patients in the T2S group experienced a 54% increase in the rate of gout flares. Conclusions: Our study is the first randomized trial to directly compare T2T with T2S as a control group in gout. We were able to show the superiority of the T2T management approach in gout.

12. Inhibition of Urate Transporters and Insulin-Activated Urate Transport by SGLT2 Inhibitors

Asim K. Mandal and David B. Mount

Brigham and Women's Hospital, Harvard Medical School, Boston, MA 02115, USA

Abstract: Background: Sodium–glucose cotransporter 2 inhibitors (SGLT2i) have well-established uricosuric and urate-lowering effects, with protective effects on gout. The mechanism(s) of these uricosuric effects is not clear, however, and direct effects on urate transporters have not been fully investigated. We report the effects of empagliflozin, canagliflozin, and dapagliflozin on urate transport in a human proximal tubular cell line and in *Xenopus* oocytes expressing individual urate transporters. Methods: We carried out Western blotting, in vitro transcription of cRNA from cloned cDNA, and urate transport assays in human renal proximal tubule epithelial cells (PTC-05) and *Xenopus laevis* oocytes expressing individual human urate transporters. Results: SGLT2 inhibitors significantly inhibited net urate uptake in a dose-dependent manner in human PTC-05 cells, which express endogenous SGLT2 and the urate transporters GLUT9a, GLUT9b, OAT10, OAT1, NPT1, ABCG2 and ABCC4. In the *Xenopus laevis* oocyte expression system, these inhibitors significantly inhibited the basal urate transport activities of URAT1, OAT10,

OAT3 and ABCC4 but not GLUT9, OAT1, and ABCG2. OAT10 was only modestly sensitive to empagliflozin and canagliflozin (~X% inhibition with 500 μM canagliflozin). For URAT1, the IC50s for empagliflozin, canagliflozin, and dapagliflozin were 460, 230, and 487 μM, respectively; for OAT3, the IC50s were 42, 29, and 21 μM, respectively. In addition, SGLT2i inhibited insulin-induced stimulation of urate transport in PTC-05 cells, with dose-dependent inhibitory effects on insulin-induced phosphorylation of the downstream Akt and ERK kinases. Conclusions: The results indicate that the uricosuric action of SGLT2 inhibitors is at least partially the consequence of impairment of the basal activities of the apical urate reabsorptive transporters URAT1 and OAT10. Additionally, SGLT2 inhibitors inhibited insulin-activated transport in a human proximal tubular cell line, with attenuated phosphorylation of Akt and ERK.

13. Transcriptomic Analysis Reveals a Proinflammatory Signature in Gout and Hyperuricemia

Valentin Nica [1], Medeea Badii [1,2], Georgiana Cabău [1], Orsolya Gaal [1,2], Andreea-Manuela Mirea [1], Ioana Hotea [3], HINT Consortium, Cristina Pamfil [3], Simona Rednic [3], Radu A. Popp [1], Yang Li [2,4], Tania O. Crișan [1,2] and Leo A.B. Joosten [1,2]

1 Department of Medical Genetics, UMF "Iuliu Hatieganu", 400012 Cluj-Napoca, Romania
2 Department of Internal Medicine, Radboud University Nijmegen Medical Center, 6525 Nijmegen, The Netherlands
3 Department of Rheumatology, UMF "Iuliu Hatieganu", 400012 Cluj-Napoca, Romania
4 Helmholtz Centre for Infection Research, 30625 Hannover, Germany

Abstract: Introduction: Gout is one of the most common inflammatory arthritis characterized by deposits of monosodium urate crystals in the joint, with an infiltration of neutrophils and macrophages. Circulating monocytes have been shown to play a critical role in rheumatic disease, as local inflammation is often driven not by local macrophages but by differentiated monocytes. Furthermore, gout is preceded by hyperuricemia, which despite being an asymptomatic condition is associated with cardiovascular comorbidities. We performed a bulk RNA-seq analysis of circulating blood cells in volunteers with various level of serum urate and gout patients to identify the signature associated with the two conditions. Methodology: Peripheral blood was harvested from volunteers and patients with gout and PBMCs were isolated within the first hour. From a subset of the same patients, CD14 monocytes were further isolated. Cells were then stored in TRIzol, and RNA-seq analysis was performed. After quality control, a total of 197 PBMC (106 normouricemic, 20 hyperuricemic, 71 gout) samples and 30 CD14 monocyte (15 normouricemic, 15 gout) samples remained. DESeq2 (R) was used to identify differentially expressed genes (DEGs). The analysis was performed both including sex and age as covariates, and separated by sex. Gene set enrichment analysis was performed with fgsea package (R), using a pre-ranked list, and transcription factor (TF) enrichment analysis was performed with chea3 (web tool). Findings: We observed a very similar transcriptomic signature in PBMCs when examining asymptomatic hyperuricemic and gout patient samples compared to normouricemic controls, which was further validated in the monocyte dataset. The most consistent DEGs across all datasets were LTF, MMP9, IL1R2, DEFA1B, SLC4A1, CEACAM8 and CYP4F3. The main upregulated pathways were related to the innate immune system, neutrophil activity and activation of matrix metalloproteinases. The top observed TFs were LTF, GATA1 and CEBPE. Furthermore, when the study groups were split by gender, males showed close to no DEGs in both comparisons, but in females, we observed the same signature with higher fold changes. A significant overlap between the examined DEGs and the sex-specific signature was observed. **Conclusions:** This study showed a proinflammatory phenotype in circulating immune cells that can be observed in some individuals, the number of which was overrepresented in both gout and asymptomatic hyperuricemia. While the cause requires further examination, we provide important insight into the pathophysiology of gout and link hyperuricemia to pathways relevant for other inflammatory diseases such as atherosclerosis. Interestingly, sex-specific differences were observed in line with a bigger

change in proinflammatory reprograming in women compared to men, further enforcing the importance of sex-specific analyses in in gout and hyperuricemia.

14. Prevalence and Factors Associated with Calcium Pyrophosphate Arthritis (CPPA) in Patients with Gout

Ana Maria Herrero-Beites and Fernando Perez-Ruiz

Rehabilitation Division, Gorliz Hospital and Rheumatology Division, Cruces University Hospital, 48903 Barakaldo, Spain

Abstract: Background: persistence of flares in patients with gout after proper treat-to-target treatment approach raise the question of whether coexistence of a disease with similar clinical characteristics could be at work, namely "pseudogout". Aim: to ascertain the prevalence of CPPA at diagnosis and during follow-up of patients with gout. Method: We assessed the data from an inception cohort of patients with gout prospectively followed-up from Jan 1994 to Dec 2023 (30 years). Gout cases were defined as crystal-proved tophus or arthritis, or presence of tophus plus double contour with ultrasonography. CPPA was defined as the presence of intra-leukocyte CPP crystals in synovial fluid (SF) and neat chondrocalcinosis in the same or a different joint. Age, gender, flares, joint distribution, previous treatment, prescribed treatment, comorbidities (hypertension/hyperlipidemia/diabetes), use of diuretics, renal function, and previous vascular disease were available for analysis. Results: A total of 1544 patients with gout, with an average of 4-year follow-up (1 month to 32 year) were available for analysis. CPPA was observed in 127 cases (8.2%); 37/1544 patients or 37/1224 synovial fluid samples (2.4% and 3.0%, respectively) showed CPP and urate crystals in the same synovial sample (cousins-not-brothers image), and 90/1544 (5.8%) patients showed CPP crystals apart from the diagnosis of gout. A total of 3 had a previous diagnosis, and 60/90 (66.6%) a diagnosis after the first 5-year period of follow-up. CPPA–gout cases referred more flares per year (3.59 vs. 3.82, $p = 0.087$) but no more polyarticular involvement at baseline (81/1007, 8.0% vs. 46/537, 8.6%, $p = 0.911$), compared to non-CPPA. In bivariate analysis, CPPA–gout cases were older at baseline (72 ± 11 vs. 61 ± 13 years). Women (20/148, 3.5% vs. 107/1396, 7.7%), patients using diuretics (72/546, 13.7% vs. 55/1018, 5.4%), patients with hypertension (102/884 6.6% vs. 25/660, 1.6%), and patients with previous vascular events (64/514, 12.5% vs. 63/1030, 6.1%) were more frequently affected. Ethanol intake over 15 g/d was apparently protective (26/479, 5.4% vs. 101/1065, 9.5%). Other variables were not associated, and multivariate analysis showed that only age and diuretics were independently associated with CPPA. Interestingly, an analysis of the prevalence in the three decades available showed an increase in CPPA diagnosis: 18/454 (4%), 50/543 (9.2%), and 59/547 (10.8%). Finding CPP and urate crystals in the same sample was also increasingly common (0/436, 13/420 (3.1%), and 24/368 (6.5%), respectively) in the first, second, and third decade. Conclusions: (1) CPPA is not infrequent in patients with gout; (2) it is associated to aging and diuretic use; (3) most patients with CPPA–gout flared after 5-year proper control, inducing a suspicion of an associated disease; and 4) joint aspiration and careful evaluation of SF are recommended in such patients.

15. Evaluation of Urate Monitoring in Gout: An Extension of the GoutSMART Supported Self-Management Trial

Philip L Riches, Debbie Alexander, Amrey Krause

NHS Lothian/University of Edinburgh, Edinburgh EH8 9YL, UK

Abstract: Background. Improved gout outcomes are associated with reduced urate levels, leading many guidelines to recommend regular urate monitoring for patients on urate-lowering therapy. We have developed a supported self-management approach to gout incorporating self-testing of urate and shown that this leads to improved attainment of urate targets within 6 months. There is a lack of evidence evaluating the impact of urate monitoring on clinical outcomes in gout, and we aimed to determine whether 2-monthly monitoring with our approach resulted in better clinical outcomes than annual monitoring.

Methods. This study was an extension of a feasibility trial in which 60 patients requiring urate-lowering therapy escalation were randomised 2:1 to supported self-management or usual care [1]. Participants from the self-management arm were offered continued 2-monthly monitoring of urate, and usual care participants were allocated to annual monitoring. Additional participants with gout on urate-lowering therapy were randomised 1:1 to either arm. All participants were provided with urate meters, and those with baseline raised urate were titrated remotely using a smartphone app (GoutSMART) to a urate target of 0.3 mmol/L. Promptd to perform 2-monthly monitoring and feedback on results were also mediated through the app. Urate-lowering therapy de-escalation was permitted in the close monitoring arm once remission had been achieved with a goal of maintaining urate $\leq$0.36 mmol/L. The primary outcome was the percentage of participants achieving a urate target $\leq$0.36 mmol/L at 24 months upon intention-to-treat analysis. The trial was registered with ClinicalTrials.gov identifier NCT03274063 (https://clinicaltrials.gov/study/NCT03274063). Results. Between September 2020 and September 2021, 67 patients were enrolled. The mean age was 55.5 years (SD 14.0); 62 (92.5%) of the participants were male, and 5 (7.5%) were female. Some 62 (92.5%) were white. A total of 40 participants were allocated to 2-monthly monitoring (30 (75%) participants from the self-management arm and 10 further recruits) and 27 participants to annual monitoring (15 (75%) participants from the usual care arm and 12 additional recruits). At 24 months, a urate level of $\leq$0.36 mmol/L was achieved by 38 (95%) participants in the 2-monthly monitoring group, compared to 17 (62.9%) participants in the annual monitoring group (risk difference 0.32 (95% CI 0.10 to 0.54); p = 0.0001). Secondary study outcomes are summarised in Table 4. Significant improvement in flare rates were associated with 2-monthly monitoring, with only 3 (7.5%) out of 39 completing the trial in the close monitoring group suffering flares in year two compared to 7 (33%) out of 21 in annual monitoring. No difference in the prescribed dose of allopurinol was seen, which is consistent with this benefit arising from improved medication compliance. Higher prescription rates for urate-lowering therapy amongst the 2-monthly monitoring arm provided objective evidence for this interpretation. A total of 7 (10.4%) participants did not complete the trial (including 2 deaths), with most (6/7) being from the annual monitoring arm, which will have influenced the primary intention-to-treat analysis. Overall, no significant difference in serious adverse events was seen. Interpretation. Supported self-monitoring of urate every 2 months resulted in improved maintenance of urate targets after 2 years when compared with annual monitoring. More frequent urate monitoring is associated with a high proportion of participants becoming flare-free, most likely due to improved compliance with medication. Our results support recommendations to monitor urate in patients prescribed urate-lowering therapy.

Table 4. Categorical study outcomes.

A								
	Year 1				Year 2			
Characteristic	**Active Care (n = 40)**	**Usual Care (n = 27)**	**Rate Difference**	**p Value**	**Active Care (n = 40)**	**Usual Care (n = 27)**	**RD**	**p Value**
Urate $\leq$ 0.36 mmol/L	35/40 (87.5%)	23/27 (85.2%)	0.02 (−0.16 to 0.21)	1.00	38/40 (95%)	17/27 (62.9%)	0.32 (0.10 to 0.54)	0.0021
Tophaceous disease	9/40 (22.5%)	7/27 (25.9%)	−0.03 (−0.27 to 0.20)	0.78	8/40 (17.5%)	6/27 (22.2%)	−0.05 (−0.27 to 0.17)	1.00
Any flares in past 12 months	18/38 (47%)	15/25 (60%)	−0.13 (−0.39 to 0.13)	0.44	3/39 (7.691%)	7/21 (33.3%)	−0.26 (−0.48 to −0.03)	0.024
Stopped treatment	0/38	0/25	0 (0)	0	0/39	2/21 (9.52%)	−0.10 (−0.22 to 0.03)	0.11

Table 4. *Cont.*

B								
	Year 1				Year 2			
Characteristic	**Active Care (*n* = 38) ***	**Usual Care (*n* = 25) ***	**Mean Difference (95% CI)**	***p* Value**	**Active Care (*n* = 39) ***	**Usual Care (*n* = 21) ***	**Mean Difference (95% CI)**	***p* Value**
Urate (mmol/L)	0.29 (0.07)	0.28 (0.06)	0.010 (−0.024 to 0.044)	0.56	0.25 (0.07)	0.28 (0.08)	0.03 (−0.010 to 0.070)	0.14
Allopurinol dose (mg/day)	421 (196)	460 (129)	39.00 (−49.97 to 127.97)	0.38	405 (163)	419 (169)	14.00 (−75.45 to 103.45)	0.76
Prescriptions issued (Days/Yr)	336.81 (62.5)	299.70 (85.04)	37.11 (1.35 to 72.86)	0.042	348.97 (91.75)	274.43 (101.63)	74.54 (26.87 to 122.26)	0.003
C								
Characteristic	**Active Care (*n* = 38)**	**Usual Care (*n* = 25)**	**Rate Difference (95% CI)**	***p* Value**	**Active Care (*n* = 39)**	**Usual Care (*n* = 21)**	**Rate Difference (95% CI)**	***p* Value**
Flares	0.79 (1.26)	1.60 (1.78)	−0.81 (−1.34 to −0.28)	0.0034	0.077 (0.27)	0.62 (1.02)	−0.54 (−0.81 to −0.27)	0.0001

Reference

1. Riches, P.L.; Alexander, D.; Hauser, B.; Kuske, B.; Krause, A.; Evaluation of supported self-management in gout (GoutSMART): a randomised controlled feasibility trial. *Lancet Rheumatol.* **2022**, *4*, e320–e328.

16. Development of a Deep Learning Model for Automated Detection of Calcium Pyrophosphate Deposition on Hand Radiographs

Elisabeth Rosoux [1], Thomas Hügle [1], Tobias Manigold [2], Guillaume Fahrni [1], Deborah Markham [3] and Fabio Becce [1]

[1] Lausanne University Hospital (CHUV) and University of Lausanne, Radiology, 1005 Lausanne, Switzerland
[2] Inselspital, Bern University Hospital and University of Bern, Rheumatology, 3010 Bern, Switzerland
[3] On behalf of Lausanne University Hospital (CHUV) and University of Lausanne, Rheumatology, 1005 Lausanne, Switzerland

Abstract: Background: Identifying the presence of calcium pyrophosphate deposition (CPPD) on large radiograph datasets for epidemiological studies is labor-intensive and limited by moderate inter- and intra-observer reliability. Here, we aimed to develop a deep learning approach for automatically and reliably detecting CPPD on hand radiographs in patients with various rheumatic diseases including gout and rheumatoid arthritis, focusing on the triangular fibrocartilage complex (TFCC) and second and third metacarpophalangeal joints (MCP-2, MCP-3) according to the 2023 ACR/EULAR classification criteria. Methods: Two radiologists independently labeled a dataset of 926 hand radiographs, yielding 319 CPPD-positive and 607 CPPD-negative cases across the three sites of interest. CPPD presence was then predicted using a convolutional neural network. The model performance was assessed using the area under the receiver operating characteristic (AUROC), sensitivity, specificity, and balanced accuracy, with heatmaps (Grad-CAM) aiding in case discrimination. Results: The algorithm for combined TFCC, MCP-2, and MCP-3 classification showed robust performance with an AUROC of 0.89 and a balanced accuracy of 0.79 (sensitivity of 0.94 and specificity of 0.65). The TFCC-alone, MCP-2-alone, and MCP-3-alone models also showed a good performance with an AUROC of 0.85, 0.81, and 0.86 and a slightly

lower balanced accuracy of 0.76, 0.67, and 0.70, respectively. Heatmap analysis revealed activation in the regions of interest for positive cases (true and false positives), but unexpected highlights were encountered possibly due to correlated features in different hand regions. Conclusions: This study highlights the potential of an automated model for CPPD detection on hand radiographs with high performance in the combined and TFCC-alone models. The MCP-2-alone and MCP-3-alone models showed lower accuracy due to class imbalance. This algorithm could, for example, be used to screen large clinical databases or electronic medical records for CPPD cases. Future work includes dataset expansion, threshold optimization, preprocessing refinement, and validation with external datasets.

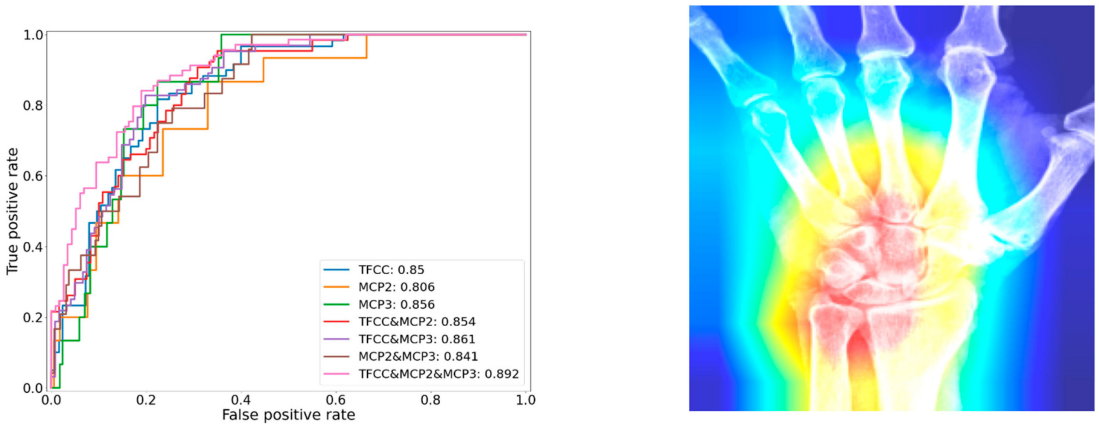

(**a**) (**b**)

Figure 7. (**a**) ROC curves (5-fold cross-validation) for the seven different potential CPPD models. (**b**) An interpretability plot (heatmap) for the combined model (TFCC-positive; MCP-2- and MCP-3-negative).

Disclosure of interest: Elisabeth Rosoux: none declared; Thomas Hügle: Roche, Novartis, BMS, GSK, Janssen, Galapagos, Atreon, Vtuls; Tobias Manigold: none declared; Guillaume Fahrni: none declared; Deborah Markham: none declared; Fabio Becce: Horizon Therapeutics.

17. Elucidating the Pathogenicity of Calciprotein Particles in Osteoarthritis

Roderick H.M.J. Stassen [1,*], Guus G.H van den Akker [1], Marjolein M.C Caron [1] and Tim J.M. Welting [1,2]

[1] Laboratory for Experimental Orthopedics, Maastricht University, 6211 Maastricht, The Netherlands
[2] Department of Orthopedic Surgery, Maastricht University Medical Center, 6211 Maastricht, The Netherlands
* Correspondence: r.stassen@maastrichtuniversity.nl

Abstract: Our objective was to characterize pCPP- and sCPP-induced changes in the human OA articular chondrocyte protein secretome in order to study their pathological role in OA and compare this to the BCP-induced protein secretome. Status: The pathobiological role of calcium-containing crystals has become inseparable from osteoarthritis (OA). In order to prevent ectopic calcification, proteins such as alpha-2 HS glycoprotein (AHSG) bind amorphous calcium phosphate particles to facilitate their clearance. These protein-bound calcium phosphate species can be categorized into primary (pCPP) and secondary calciprotein particles (sCPP), based on their distinct maturation characteristics. Presence of hydroxyapatite and increased AHSG [4] in OA synovial fluid strongly hints at the presence of CPPs. However, their pathobiological contribution remains yet to be elucidated. Methodology: BCP crystals were produced as previously described [5]. Calciprotein particles were prepared in calcium and phosphate-enriched culture medium as previously

described [3]. pCPP formation was allowed for 24 h and sCPP for 7 days, both in the presence of 10% FCS. Characterization was performed by transmission electron microscopy and nanoparticle tracking analysis. Human OA articular chondrocytes (OA-HACs) were isolated from total knee replacement surgical waste material (METC 2017-0183). OA-HACs from eight individual donors were stimulated with 50 μg/mL of either of the three particle species for 24 h. Conditioned medium samples from these cultures were analyzed for expression of soluble proteins using antibody arrays (Raybiotech L1000) or ELISA. Differential expression was determined considering fold-change (FC) >1.25 and <0.8 with $p \leq 0.05$. Findings: BCP crystals showed a well-defined crystal structure of approximately 123 nm in size, while pCPPs presented as spherical particles with an average size of 144.5 nm. sCPPs were characterized by spikey protrusions with needle-like shapes with an average size of 143.3 nm (Figure 8A). This is in line with earlier reported characteristics [2]. Exposure of OA-HACs to BCP crystals increased their IL-6 and PGE_2 secretion. pCPPs did not increase secretion of IL-6. However, sCPPs did induce secretion of these factors but were less potent provoking this compared to BCP crystals (Figure 8B). Protein secretome analysis unveiled the full extent of differential OA-HAC responses between the three different particles. BCP crystal stimulation resulted in 26 differentially expressed (DE) proteins, of which 4 were up- and 22 downregulated with respect to the non-treated control condition. The highest upregulated protein was Activin A (FC = 3.35), and the most downregulated protein CBR1 (FC = 2.08). Although pCPPs did not induce secretion of IL-6 or PGE_2, we found 56 DE proteins, of which 42 proteins were significantly up and 14 downregulated by pCPPs compared to control. Furthermore, 49 DE proteins were found in response to sCPP crystal stimulation of OA-HACs. Of these proteins, 22 were upregulated and 27 downregulated by sCPPs. In both CPP datasets, FGF-BP was the most upregulated protein (pCPP FC = 2.36 and sCPP FC = 5.23). For pCPP, we found CA125 (FC = 3.89), and for sCPP, Fibrinogen (FC = 3.61) to be the most down regulated proteins. Other DE proteins that we identified were, among other processes, involved in cell chemotaxis, ossification, and angiogenesis. Significance: This study for the first time characterized CPP-driven chondrocyte secretory responses. The characterization of the OA-HAC protein secretomes uncovered divergent responses between the different particle types. These results will help us to gain a better understanding of the diverse roles of calcium-containing crystals in OA pathobiology and potentially aid the development of DMOADs.

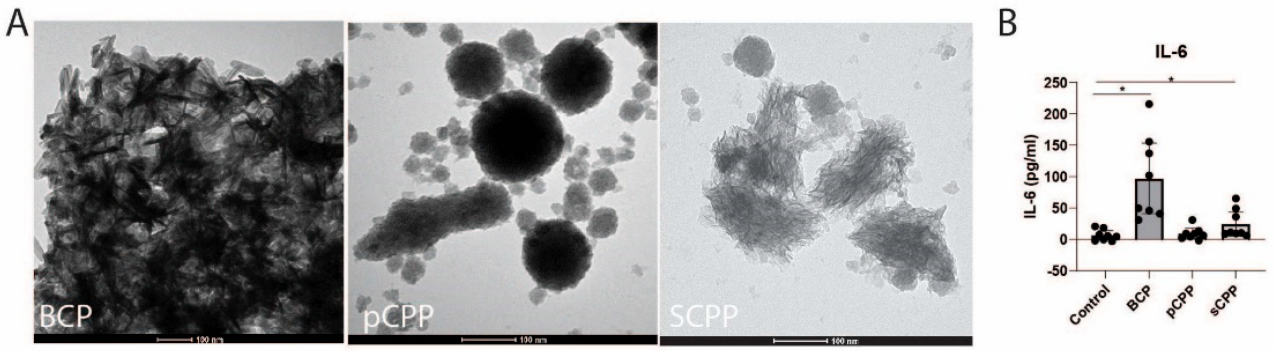

Figure 8. Differential response to BCP and calciprotein particles by human OA articular chondrocytes. (**A**) Transmission electron microscopic picture of the different calcium-containing species in the following order BCP, pCPP and sCPP. (**B**) Secreted protein levels of IL-6 by OA HACs in response to BCP, pCPP and sCPP after 24 h. Data are presented as mean ± SEM, $n = 3$ per donor. * p value < 0.05.

References

1. Yavorskyy, A.; Hernandez-Santana, A.; McCarthy, G.; McMahon, G. Detection of calcium phosphate crystals in the joint fluid of patients with osteoarthritis—analytical approaches and challenges. *R. Soc. Chem.* **2008**, *133*, 302–318.

2. Jahnen-Dechent, W.; Smith, E. Nature's remedy to phosphate woes: calciprotein particles regulate systemic mineral metabolism. *Kidney Int.* **2020**, *97*, 648–651.
3. Aghagolzadeh, P.; Bachtler, M.; Bijarnia, R.; Jackson, C.; Smith, E.R.; Odermatt, A.; Radpour, R.; Pasch, A. Calcification of vascular smooth muscle cells is induced by secondary calciprotein particles and enhanced by tumor necrosis factor-α. *Atherosclerosis* **2016**, *251*, 404–414.
4. Timur, U.T.; Jahr, H.; Anderson, J.; Green, D.C.; Emans, P.J.; Smagul, A.; van Rhijn, L.W.; Peffers, M.J.; Welting, T.J.M. Identification of tissue-dependent proteins in knee OA synovial fluid. *Osteoarthr. Cartil.* **2021**, *29*, 124–133.
5. Stassen, R.H.M.J.; van den Akker, G.G.H.; Surtel, D.A.M.; Housmans, B.A.C.; Cremers, A.; Caron, M.M.J.; Smagul, A.; Peffers, M.J.; van Rhijn, L.W.; Welting, T.J.M. Unravelling the Basic Calcium Phosphate crystal-dependent chondrocyte protein secretome; a role for TGF-β signaling. *Osteoarthr. Cartil.* **2023**, *31*, 1035–1046.

18. Differential Regulation of Pyrophosphate Metabolism in Calcified and Non-Calcified Cartilage and Synovium of Osteoarthritis Patients

Sina Stücker, Franziska Koßlowski, Adrian Buchholz, Christoph H. Lohmann and Jessica Bertrand

Department of Orthopaedic Surgery, Otto-von-Guericke-University, 39106 Magdeburg, Germany

Abstract: Objective: Calcification of articular cartilage and synovium is a common symptom in osteoarthritic knee joints and is closely related to the progression of the disease. Involved crystal types are difficult to identify and differentiate, resulting in inconsistent data on the prevalence and distribution of calcified deposits. Extracellular phosphate and pyrophosphate levels play an important factor in the formation of different crystal types and are regulated by various metabolizing enzymes. This study analyses BCP and CPP calcifications in cartilage and synovium of OA patients undergoing knee replacement surgery. Methodology: Combining multiple imaging methods including conventional radiography, histology and Raman spectroscopy, this study provides a comprehensive analysis of BCP- and CPP-based calcification and its frequency and distribution in cartilage and synovial membrane samples of 94 OA patients undergoing knee replacement surgery. To elucidate the process of BCP and CPP formation, we investigated the regulation of the phosphate metabolism by measuring the gene expression, protein expression, and activity of various phosphatases and nucleotidases using qRT-PCR, immunohistochemistry and colorimetric activity assays. Findings: 35% of patients displayed radiologically detectable calcifications. Histological analysis revealed calcifications in 88% of cartilage and 57% synovial samples. Here, BCP crystals usually formed variably sized deposits of brittle appearance, located on the cartilage surface or within synovial tissue. In contrast, CPP crystals accumulated in larger needle-shaped clusters, condensing to circular pockets below the cartilage surface or within synovial tissue. Raman spectroscopy detected BCP crystals in 75% of cartilage and 43% of synovial samples. Merely 18% of cartilage and 15% of synovial samples contained CPP crystals, often in the vicinity of BCP deposits. Gene expression levels of alkaline phosphatase (ALP), ectonucleotide pyrophosphatase/phosphodiesterase 1 (ENPP1), ankylosis homologue (ANKH), and 5′-nucleotidase (CD73) were increased in BCP-calcified compared to non-calcified cartilage. However, we could not detect differences in gene expression in BCP- versus CPP-calcified cartilage. Expression levels in synovium did not differ either. On the protein level, we could not detect significant differences in ALP, ENPP1, ANKH or CD73 expression in BCP- compared to CPP-calcified cartilage or synovium. The activity levels of NPP1 and ALP were decreased in calcified compared to non-calcified cartilage, whereas inorganic phosphate levels were increased. Significance: Calcifications in cartilage and synovium in OA patients are predominantly caused by BCP crystals. CPP deposition is rare and often located in proximity to BCP deposits. Distinguishable morphological characteristics and distribution patterns of BCP and CPP crystals may suggest the involvement of different underlying diseases or endotypes that might require different treatment strategies.

The similar gene and protein expression and activity levels of ALP, ENPP1, and ANKH in BCP- and CPP-calcified joint tissues suggest that additional factors may dictate the type of crystal formation.

19. Correlation of Circulatory Mineralization Factors with Alkaline Phosphatase Activity upon Aging in Mice and Humans

Virgil Tamatey [1,2], Martin Várhegyi [1,3], Dániel Kovács [1], Dénes Juhász [4], Anikó Ilona Nagy [4], Tamás Arányi [1] and Flora Szeri [1]

1 HUN-REN Research Centre for Natural Sciences, Institute of Molecular Life Sciences, 1117 Budapest, Hungary
2 Doctoral School of Biology, ELTE, H-1053 Budapest, Hungary
3 Doctoral School of Semmelweis University, 1085 Budapest, Hungary
4 Heart and Vascular Center, Semmelweis University, 1085 Budapest, Hungary

Abstract: Tissue-nonspecific alkaline phosphatase is primarily expressed in the liver and bone but is also present in the circulation in a soluble form. Serum alkaline phosphatase (AP) cleaves the mineralization inhibitor inorganic pyrophosphate (PPi) to inorganic phosphate (Pi), a building block for biominerals. Plasma PPi is an essential inhibitor of ectopic calcification in acquired conditions, e.g., chronic kidney disease, and in rare hereditary mineralization disorders such as pseudoxanthoma elasticum (PXE). PXE manifests due to loss of function mutations in ABCC6, resulting in 70–50% reduced plasma PPi levels compared to controls. As the kinetics and determinants of extracellular PPi homeostasis are largely unknown, we investigated the circulatory AP-PPi-Pi axis in *Abcc6*$^{-/-}$ and wild-type (WT) mice and control human individuals with no CT-detectable ectopic calcification. We found profound changes in the AP activity, PPi, and Pi levels during maturation and aging in mice. AP activity is high at weaning but drastically declines at a young age, paralleled with up to a twofold increase in plasma PPi levels in both WT and *Abcc6*$^{-/-}$ strains. Later in life, plasma PPi of *Abcc6*$^{-/-}$ mice steadily increase while Pi, and consequently the Pi/PPi ratio, an important determinant of the calcification propensity, decreases. In the *Abcc6*$^{-/-}$ mice, AP activity exhibits a strong negative and modest positive correlation with PPi and Pi levels, respectively, up to 600 days; thus, the Pi/PPi ratio strongly correlates to serum AP activity. Human control individuals with no CT-detectable coronary and heart valve calcification exhibit similar kinetics, with a significant age-dependent increase in plasma PPi and a decrease in the Pi/PPi ratio. Moreover, plasma PPi levels and circulatory Pi/PPi ratio strongly correlate to AP activity. Our data hint that AP activity plays a role in determining circulatory PPi and Pi levels in mice and humans under certain circumstances. Consequently, the Pi/PPi balance is altered over a lifetime, favoring mineralization in the young and acting against calcification in the elderly through a putative preventive mechanism likely independent of ABCC6 function.

20. Overlap of Gout Variants with Activity-by-Contact (ABC) Enhancers in Stimulated Innate Immune Cells Reveals *CSF1* and *CSF1R* Genes Involved in Gout Inflammation

Riku Takei *, Megan P. Leask, and Tony R. Merriman

Division of Clinical Immunology and Rheumatology, University of Alabama at Birmingham, Birmingham, AL 35294, USA
* Correspondence: rikutakei@uabmc.edu

Abstract: Objective: Activity-By-Contact (ABC) enhancers identify enhancer regions that physically connect to a gene promoter region [1]. Using ABC enhancer data, we investigated whether immune cell-related ABC enhancers in stimulated innate immune cells overlap with genetic loci identified in a genome-wide association study (GWAS) of gout. Methodology: An ABC enhancer–gene connection dataset [1] was downloaded. ABC enhancer regions were restricted to those with an ABC score of $\geq$0.015 [1] and from 57 (31 stimulated and 26 unstimulated) immune cells or cell-lines. Lead variants from a gout GWAS [2] were tested for genetic colocalization (using the "coloc" package in R [3]) with a

Genotype–Tissue Expression (GTEx) [4] quantitative trait loci (eQTL) dataset to identify variants that may affect risk of gout via gene expression. The threshold for posterior probability for hypothesis 4 (PPH_4) was set at $\geq$0.8, which indicates strong evidence of shared signal between gout and the eQTL. The eQTL-colocalized gout variants were overlapped with the ABC enhancer regions to assess whether the variants lay within the ABC enhancers. Results: Of the 340 lead gout variants tested, 273 variants (80.3%) genetically colocalized ($PPH_4 \geq 0.8$) with eQTL for at least one gene in *cis* or *trans*. In total, 29 variants (10.6%) that colocalized with eQTL were within an ABC enhancer region for 177 genes. For stimulated innate immune cells and cell lines, 14 variants were within an ABC enhancer for 85 genes. Among these genes was *CSF1*, where the lead gout variant rs2938616 is within an ABC enhancer region for the gene and also a colocalized eQTL of *CSF1*. In addition to *CSF1*, *CSF1R* also had a lead gout variant (rs2282804) within its ABC enhancer region, although it did not colocalize with an eQTL for *CSF1R*. ABC enhancer regions for both *CSF1* and *CSF1R* were exclusive to stimulated innate immune cells. Conclusions: Through enhancer activity estimates and three-dimensional connection frequencies, ABC enhancers provide valuable information on how a gene may be regulated. Acute gout inflammation results from an innate immune response to monosodium urate (MSU) crystals. By focusing on stimulated innate immune cell types, we were able to identify gout eQTL variants that were within an ABC enhancer, indicating that these genes may be regulated through these enhancer regions in immune cell types. In particular, the gene for colony-stimulating factor 1, *CSF1*, was amongst the genes that had colocalized eQTL and the promoter was contacted by an ABC enhancer region for the same gene. *CSF1* controls the differentiation and proliferation of monocytes and macrophages [5], indicating its possible role in gouty inflammation. In addition to *CSF1*, its receptor, *CSF1R*, showed evidence of ABC enhancer–gene connections, and the ABC enhancer regions for both *CSF1* and *CSF1R* are binding sites for the transcription factors nuclear factor kappa B (NF-κB) and repressor element 1 silencing transcription factor (REST). A recent study of gout in an adolescent Chinese cohort[6] showed that genetic association with REST corepressor 1 (RCOR1) and suppression of REST expression reduced the production of pro-interleukin-1β (pro-IL-1β) in THP-1 cells after MSU crystal stimulation, further supporting the potential involvement of *CSF1/CSF1R* in gouty inflammation.

References

1. Nasser, J.; Bergman, D.T.; Fulco, C.P.; Guckelberger, P.; Doughty, B.R.; Patwardhan, T.A.; Jones, T.R.; Nguyen, T.H.; Ulirsch, J.C.; Lekschas, F.; et al. Genome-wide enhancer maps link risk variants to disease genes. *Nature* **2021**, *593*, 238–243.
2. Major, T.J.; Takei, R.; Matsuo, H.; Leask, M.P.; Topless, R.K.; Shirai, Y.; Li, Z.; Ji, A.; Cadzow, M.J.; Sumpter, N.A.; et al. A genome-wide association analysis of 2,622,830 individuals reveals new pathogenic pathways in gout. *medRxiv* **2022**. https://doi.org/10.1101/2022.11.26.22281768.
3. Giambartolomei, C.; Vukcevic, D.; Schadt, E.E.; Franke, L.; Hingorani, A.D.; Wallace, C.; Plagnol, V. Bayesian Test for Colocalisation between Pairs of Genetic Association Studies Using Summary Statistics. *PLOS Genet.* **2014**, *10*, e1004383.
4. GTEx Consortium. The Genotype-Tissue Expression (GTEx) project. *Nat. Genet.* **2013**, *45*, 580–585.
5. Sehgal, A.; Irvine, K.M.; Hume, D.A. Functions of macrophage colony-stimulating factor (CSF1) in development, homeostasis, and tissue repair. *Semin. Immunol.* **2021**, *54*, 101509.
6. Ji, A.; Sui, Y.; Xue, X.; Ji, X.; Shi, W.; Shi, Y.; Terkeltaub, R.; Dalbeth, N.; Takei, R.; Yan, F.; et al. Novel genetic loci in early-onset gout derived from whole genome sequencing of an adolescent gout cohort. *Arthr. Rheum.* **2024**. https://doi.org/10.1002/art.42969.

21. Integrative Analysis Reveals the Multilateral Inflammatory Mechanisms of CD14 Monocytes in Gout

Ahmed Alaswad [1,2], Georgiana Cabău [3], Tania O. Crişan [3,4], Liang Zhou [1,2], Martijn Zoodsma [1,2], HINT Consortium [3], Mihai G Netea [4,5], Cheng-Jian Xu [1,2] Yang Li [1,2,*,†] and Leo A. B. Joosten [3,4,†]

1 Department of Computational Biology for Individualized Infection Medicine, Centre for Individualized Infection Medicine, A Joint Venture between the Hannover Medical School and the Helmholtz Centre for Infection Research, 30625 Hannover, Germany
2 TWINCORE, Centre for Experimental and Clinical Infection Research, A Joint Venture between the Hannover Medical School and the Helmholtz Centre for Infection Research, 30625 Hannover, Germany
3 Department of Medical Genetics, Iuliu Hatieganu University of Medicine and Pharmacy, 400349 Cluj-Napoca, Romania
4 Department of Internal Medicine and Radboud Institute for Molecular Life Sciences, Radboud University Medical Center, 6525 Nijmegen, The Netherlands
5 Department of Immunology and Metabolism, Life and Medical Sciences Institute (LIMES), University of Bonn, 53115 Bonn, Germany
* Correspondence: yang.li@helmholtz-hzi.de
† Authors share the last authorship.

Abstract: Background/Objectives: Gout, a prevalent inflammatory arthritis, is associated with urate crystal deposition and immune cell activation. However, the precise contribution of immune cells, specifically CD14 monocytes, in initiating this inflammatory disease remains a pivotal and evolving inquiry. Using single-cell transcriptomes of patients and controls from multiple cohorts, this study utilized an integrative approach to robustly characterize the molecular and cellular landscapes of CD14 monocytes in gout. Furthermore, the study examined the intersection of the identified gout transcriptome with in vitro monosodium urate (MSU)-induced genes or with genes prioritized for a potential role in inflammation by the most recent gout GWAS, shedding light on different angles to deepen the understanding of CD14 monocyte's role in this disease. Status: the project is currently in the manuscript drafting stage. Methodology: In this cross-sectional case-control study, peripheral blood mononuclear cells (PBMCs) were collected from eight patients with gout and six healthy donors (discovery group). The collected PBMCs were subjected to scRNA sequencing to characterize their transcriptome profile. We used different supporting online data to replicate, validate, or explain the findings from the discovery group. Findings: At the molecular level, we previewed how *HIF1A* and hypoxia-related pathways are heavily involved in regulating IL-1b production from CD14 monocytes in gout. We also recorded the significant downregulation of *CLEC12A* expression along all CD14 monocyte subclusters. At the cellular level, we identified the S100A^{high} CD14 monocyte subcluster, which we found responsible for NLRP3 and CLEC7 inflammasome pathways as well as prostaglandin secretion from CD14 monocytes in gout. Furthermore, upon examining the in vitro MSU-induced differentially expressed genes (DEGs), we found high enrichment and consistency with the S100A^{high} CD14 monocyte gout-enriched DEGs, confirming how these two arms jointly build up inflammation in gout. Finally, GWAS-prioritized genes highlighted the importance of fatty acid metabolism, ending with significant enrichment of the prostaglandin excretion pathway from S100A^{high} CD14 monocytes in gout, a finding that we can also replicate using public data. Significance: This study advanced our understanding of the role of CD14 monocytes in gout through a comprehensive molecular profile. The identified genes and cell subcluster markers offer promising therapeutic targets in various inflammatory or regulatory pathways, emphasizing precision medicine's potential in gout management.

22. Intra-Versus Extracellular Synovial Fluid Calcium Pyrophosphate Crystals for the Diagnosis of Acute Calcium Pyrophosphate Crystal Arthritis

David Harris [1,*], Douglas White [1,2] and Uri Arad [1,2]

1 Rheumatology Department, Waikato Hospital, Hamilton 3204, New Zealand
2 Waikato Clinical School, University of Auckland, Hamilton 3240, New Zealand
* Correspondence: david.harris@waikatodhb.health.nz

Abstract: Objective: Acute calcium pyrophosphate (CPP) crystal arthritis is characterised by the presence of CPP crystals in the synovial fluid of a clinically inflamed joint. CPP crystals can be found in an intracellular or extracellular location; however, no studies have specifically assessed the importance of the CPP crystal location in the clinical setting. The objective of this retrospective cohort study was to assess the relevance of the CPP crystal location in the diagnostic work up of acute CPP crystal arthritis. Methods: Data were collected from Waikato District Health Board (WDHB) to identify a study population with synovial fluid samples positive for CPP crystals. Two cohorts were identified, one with intracellular and one with extracellular CPP crystals. The proportion of cases diagnosed with acute CPP crystal arthritis, according to predefined criteria, was compared between these cohorts. Further analysis was made with respect to demographics, other laboratory results, and cartilage calcification. Results: The study population consisted of 134 patients, 108 with intracellular CPP crystals and 26 with extracellular CPP crystals. Acute CPP crystal arthritis cases made up 84% of the intracellular cohort and 42% of the extracellular cohort ($p < 0.001$). When septic arthritis cases were excluded from the analysis, 96% of cases with intracellular CPP crystals were secondary to acute CPP crystal arthritis ($p < 0.001$). Conclusions: Our study suggests the presence of an intracellular CPP crystal location is more likely to be associated with acute CPP crystal arthritis. An extracellular CPP crystal location appears less specific and more likely to be an incidental finding.

23. Matrix Gla Protein Deficiency in Mice Induces Accelerated Trachea Cartilage Calcification and Reveals an Unexpected Mucosal Calcification

Elodie Baptista [1], Lina Tabcheh [1], Juliana Marulanda Montoya [2], Chaohua Deng [1], Joseph Deering [3], Jean-Yves Jouzeau [1], Arnaud Bianchi [1], Marc D. McKee [3], Monzur Murshed [2] and Hervé Kempf [1]

1 Ingénierie Moléculaire, Cellulaire et Physiopathologie, UMR 7365 CNRS-Université de Lorraine, 54000 Vandœuvre-lès-Nancy, France
2 Department of Medicine, Faculty of Dental Medicine and Oral Health Sciences, McGill University, Montreal, QC H3A 0G4, Canada
3 Department of Anatomy and Cell Biology, Faculty of Dental Medicine and Oral Health Sciences, McGill University, Montreal, QC H3A 0G4, Canada

Abstract: Introduction: Tracheal calcification is a rare condition mostly found in the elderly in which tracheal elasticity is compromised, leading eventually to dyspnea. Tracheal calcification is also found in younger individuals suffering from pathologic conditions such as Keutel syndrome (KS), a rare genetic disease caused by loss-of-function mutations in the matrix Gla protein (MGP) gene. MGP is a calcification inhibitor, and KS patients show abnormal apatitic mineral deposition in most of the cartilaginous tissues, which is accompanied by midface hypoplasia, brachytelephalangism, peripheral pulmonary stenosis, and respiratory complications including asthma, dyspnea and respiratory tract infection. In this context, we sought to understand the mechanisms underlying tracheal mineralization that so far have been unexplored and more specifically to investigate the role of MGP in this process. Material and Methods: Alcian blue/Alizarin red and Von Kossa/Alcian blue double stainings were performed on whole trachea and on 5 µm thick sections of trachea samples, respectively, at different postnatal ages (P0 to P60) in wild-type (WT, $Mgp^{+/+}$) and MGP-deficient ($Mgp^{-/-}$) mice. Collagen X expression was detected by in situ hybridization in cartilage rings and also assessed by qPCR. Sub-micron micro-computed X-ray tomography (µCT), also known as X-ray microscopy (Zeiss Xradia Versa) was also performed on

the trachea of WT and knockout mice and analyzed using Dragonfly software. Results: Our morphological and histological investigations revealed an unexpected phenomenon in WT mice, wherein tracheal calcification occurred as early as 30 days after birth. With aging, this mineralization extended in a rostro-caudal pattern along the respiratory tract, through a process involving terminal differentiation of tracheal chondrocytes overexpressing the hypertrophic marker collagen X. In MGP-deficient mice, the overall mineralization of the respiratory tract was accelerated, with calcification of tracheal cartilage rings starting at 14 days after birth. Moreover, $Mgp^{-/-}$ mice also exhibited an unexpected calcification in the tracheal mucosa, more precisely in the lamina propria, associated with a structural modification of the overlying epithelium. This calcification was restricted to the trachea and was not found in other epithelia in these knockout mice. No similar lamina propria calcification was observed in WT mice, even in very old mice (up to 24 months) in which all tracheal cartilage rings were calcified. Conclusions: The present study is the first to comprehensively describe mouse tracheal mineralization and provide evidence that calcification of the cartilage rings appears to be a sudden and early physiologic event in mice. It also demonstrates that MGP is a key factor regulating mineralization of the tracheobronchial tree. Indeed, MGP deficiency accelerates tracheal cartilage mineralization and appears responsible for an additional calcification of the trachea in the mucosal layer, which leads to changes that could explain the respiratory problems found in patients with KS who suffer from dyspnea, cough, stridor, and infections (previously attributed to tracheal ring calcification).

Keywords: trachea; calcification; matrix Gla protein

24. The Response of Ultrasound and Clinical Features of Gout in Patients Managed with a Treat-to-Target Serum Urate Protocol

David Bursill [1,2], Anita Lee [1,2], Kim Griggs [1,2], Phoebe Hunter [1,2], Emma Hocking [1,2], Leah McWilliams [1], Vidya Limaye [1,2] and Susanna Proudman [1,2]

[1] Rheumatology Unit, Royal Adelaide Hospital, Adelaide, SA, Australia
[2] University of Adelaide, Adelaide, SA, Australia

Abstract: Background: Treat-to-target (TTT) urate-lowering therapy (ULT) is an effective approach to the management of gout, and ultrasound (US) is a sensitive tool through which to detect monosodium urate (MSU) crystal deposition. We investigated the progression of and relationship between clinical and US-detected features of gout in patients undergoing TTT ULT in a protocolised outpatient clinic. Methods: Patients over 18 years with gout (defined by 2015 ACR-EULAR classification criteria) was managed with a standardised TTT ULT protocol at the Royal Adelaide Hospital. Patients were assessed at baseline, 6, and 12 months for the clinical features of gout (flares, subcutaneous tophi, tender and swollen joints, and serum urate (SU)) and US features of gout (double contour sign (DCS), tophi, hyperechoic foci (HEF), erosions, effusion, synovitis and power Doppler positivity). US sites examined included the knees, peroneus tendons, and all metatarsophalangeal (MTP) joints. Subcutaneous tophus volume (STV) was calculated (STV = [width^2 $\times$ length]/2) based on measurements taken with digital Vernier callipers. US tophus burden was calculated by summing the maximal diameter of the two largest tophi detected at each site (three largest at the knees). US evidence of effusion and synovitis was graded 0 to 3; only moderate and severe grades were used for subsequent analyses. Statistical analyses were performed using IBM SPSS Statistics (version 29.0.1.0). Data were transformed using ARTool for parametric analysis. Variable trends were evaluated using Friedman's ANOVA and Wilcoxon signed rank tests with Bonferroni-adjusted post hoc analysis, alongside a repeated-measures ANOVA. Results: A total of 50 patients (82% male, mean age 62.9 $\pm$ 14.0 years, median disease duration 9.4 (IQR 24.2) years) were included (Tables 5 and 6). At baseline, there was no significant effect of ULT duration on STV, DCS or US tophus burden. SU significantly decreased from baseline to month 6 (median 0.43 (IQR 0.18) to 0.30 (IQR 0.07) mmol/L, $p <$ 0.001), with 43.8% participants at 6 months and 60.9% at 12 months achieving the target of <0.30 mmol/L ($p < 0.001$). Flare frequency was also significantly reduced by 6 months (me-

dian 0.42 (IQR 0.7) to 0.00 (IQR 0.05) flares/month, $p < 0.001$). STV significantly decreased from baseline to month 6 (median 14.75 (IQR 42) to 0.96 (IQR 22) cm^3, $p = 0.01$, Figure 9). Correspondingly, US features of MSU crystal deposition also significantly reduced from baseline to month 6, including DCS (median 1 (IQR 2) to 0 (IQR 1) sites/patient, $p = 0.003$) and US tophus burden (median 11.85 (IQR 22.1) to 8.95 (IQR 18.2) mm, $p < 0.001$, Figure 9). US features of inflammatory arthritis did not decrease at 12 months, with no significant change in effusion (mean 7.4 (SD 2.1) to 7.4 (SD 2.6)), synovitis (median 2 (IQR 3) to 1 (IQR 1)), or power Doppler (median 0 (IQR 2) to 0 (IQR 1))-positive sites per patient (all $p > 0.05$). Ultrasound was able to detect evidence of MSU deposition ($\geq$1 tophus and/or DCS) in 27/28 (96%) patients with no clinically discernible subcutaneous tophi; limited ultrasound examination of the knees and first MTP joints detected MSU deposition in 24 (86%) of this subgroup with clinically non-tophaceous disease. Conclusions: TTT ULT can lead to early improvements in the clinical features of gout, including flares and subcutaneous tophi, which corresponds to the temporal reduction of MSU crystal deposits detected on US. US evidence of inflammation persisted at 12 months, which has implications for the disease course of this chronic inflammatory arthritis and may influence treatment decisions. US provides a valuable, non-invasive assessment of the subclinical manifestations of gout and their response to ULT.

Table 5. Baseline patient characteristics.

N (male)		50 (41)
Age (years), mean (SD)		62.9 (14.0)
BMI (kg/m^2), mean (SD)		30.2 (5.7)
Gout history		
Gout duration, median years (IQR)		9.4 (24.2)
Synovial fluid crystal diagnosis, *n* (%)		17 (34%)
Flares (in 12 months pre-baseline), median (IQR)		5.0 (8)
Duration of pre-baseline urate-lowering therapy	*n* (%)	Baseline serum urate (mmol/L), mean (SD)
<3 months: *n* (%), SU (mmol/L)	29 (58%)	0.45 (0.13)
3–12 months: *n* (%), SU (mmol/L)	12 (24%)	0.37 (0.15)
>12 months: *n* (%), SU (mmol/L)	9 (18%)	0.41 (0.10)
Clinical features of gout		
Subcutaneous tophi, *n* (%)		22 (44%)
Swollen joints, *n* (%)		27 (55%)
Tender joints, *n* (%)		26 (54%)
Comorbidities		
Chronic kidney disease:		
eGFR $\geq$ 60 mL/min/1.73 m^2, *n* (%)		32 (64%)
eGFR < 60 mL/min/1.73 m^2, *n* (%)		18 (36%)
Hypertension, *n* (%)		30 (60%)
Hypercholesterolemia, *n* (%)		21 (42%)
Type 2 diabetes, *n* (%)		10 (20%)
Diuretic therapy, *n* (%)		11 (22%)

BMI: body mass index; IQR: interquartile range; SD: standard deviation; SU: serum urate.

Table 6. Baseline ultrasound characteristics.

	Total	**Duration of Urate-Lowering Therapy Pre-Baseline ***		
		<3 Months (*n* = 29)	**3–12 Months (*n* = 12)**	**>12 Months (*n* = 9)**
Synovitis Number of joints with grade 2–3 synovitis, median (IQR)	2 (3)	2 (3)	2 (4)	1 (2)

Table 6. *Cont.*

	Total	Duration of Urate-Lowering Therapy Pre-Baseline *		
		<3 Months (*n* = 29)	3–12 Months (*n* = 12)	>12 Months (*n* = 9)
Double contour (DC) sign				
≥1 DC sign any joint, *n* (%)	34 (68%)	20 (69%)	8 (67%)	6 (67%)
≥1 DC sign knees, *n* (%)	18 (36%)	11 (38%)	5 (42%)	2 (22%)
≥1 DC sign MTP1, *n* (%)	20 (40%)	12 (41%)	3 (56%)	20 (40%)
Presence of ultrasound tophi				
≥1 tophus any joint, *n* (%)	46 (92%)	26 (90%)	11 (92%)	9 (100%)
≥1 tophus knees, *n* (%)	30 (60%)	17 (59%)	8 (67%)	5 (56%)
≥1 tophus MTP1, *n* (%)	36 (72%)	20 (69%)	7 (58%)	9 (100%)

IQR: interquartile range; DC: double contour; * no statistically significant difference ($p \geq 0.05$) between groups for synovitis, DC sign, and ultrasound tophi using Friedman's ANOVA and Wilcoxon signed rank tests.

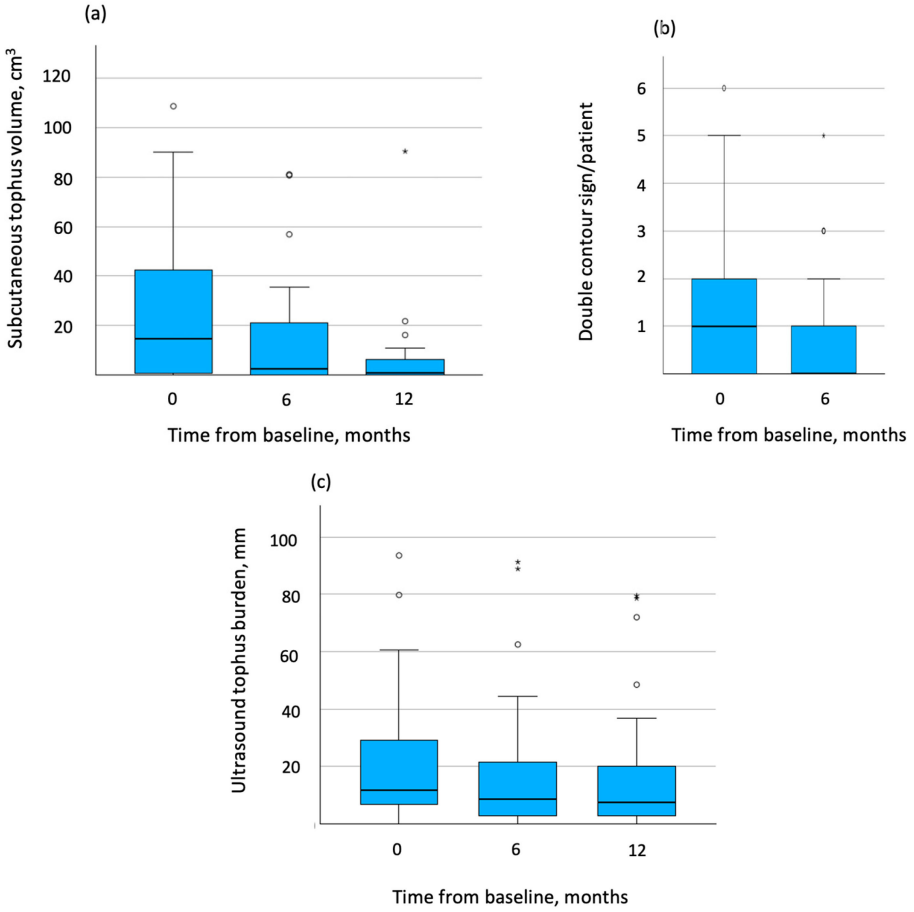

Figure 9. Subcutaneous tophus volume (**a**), double contour sign (**b**), and ultrasound tophus burden (**c**) over time following introduction of treat-to-target urate-lowering therapy.

25. Rasburicase and Methotrexate Co-Therapy in a Case of Difficult-to-Treat Gout

María Fernanda del Pino-Zambrano, Patricio Cardoso-Penafiel, Claudia María Gomez-Gonzalez and Enrique Calvo-Aranda

Hospital Universitario Infanta Leonor, 28031 Madrid, Spain

Abstract: Background: Gout is caused by the deposition of urate crystals. To dissolve deposits, serum uric acid (UA) levels should be targeted to be below 6 mg/dL (<5 in tophaceous gout) with urate-lowering treatments (ULTs) such as allopurinol, febuxostat, or benzbromarone. However, some patients are refractory or intolerant to standard treat-

ment, requiring alternative drugs, such as uricases. Rasburicase is a recombinant uricase indicated in patients with hematologic malignancies with risk of tumour lysis syndrome (hyperuricemia and acute renal failure) at the beginning of chemotherapy. It has also been successfully used off-label in difficult-to-treat (D2T) gout but may cause severe allergic reactions including anaphylaxis. Pegloticase is a uricase indicated for severe gout, but it is not currently available in Europe and may also cause infusion reactions. To reduce immunogenicity, co-therapy with methotrexate has been approved in patients with gout undergoing pegloticase treatment, based on several clinical trials. To date, this strategy has not been reported in patients treated with rasburicase. Case presentation: We assessed a 69-year-old male with chronic polyarticular tophaceous gout (Figure 10), hypertension, diabetes, ischemic heart disease, and chronic kidney disease (CKD). He had previously received colchicine, NSAIDs, and corticosteroids, with poor tolerance to four ULTs (rash with allopurinol, dizziness with benzbromarone and lesinurad, general malaise with febuxostat). Co-treatment with subcutaneous methotrexate (10 mg/week; CKD) and monthly intravenous rasburicase (0.2 mg/kg) was started, with subsequent intensification to bi-weekly administration after the first months to fasten dissolution of tophi. Blood tests were performed before and after each infusion to monitor UA and hepatic/renal function. Initially, the patient tolerated the treatment well, without significant gout attacks or relevant AEs. However, after 16 months and 22 rasburicase infusions, only a slight decrease in tophus volume was observed, despite subjective progressive improvement in joint mobility and tophus consistency. Furthermore, a progressive increase in UA levels was detected after the last infusions (Figure 11), leading to treatment discontinuation. Discussion: D2T tophaceous gout is not uncommon and poses a therapeutic challenge. In these patients, uricases can be an effective alternative, but potentially dangerous AEs have been described. Several studies have been conducted with immunomodulators such as methotrexate, which are associated with pegloticase in gout, improve response rates, and reduce allergic reactions. Nevertheless, there are no reports regarding co-therapy with methotrexate and rasburicase, the only available uricase in Europe. We present a case of D2T tophaceous gout treated with rasburicase and methotrexate. Co-therapy was well tolerated but only achieved a mild clinical response despite shortening the interval between rasburicase infusions, with a progressive increase in post-infusion UA levels, which led to the suspension of the treatment. Among the possible reasons for the lack of response and potential immunogenicity development could be the dose of methotrexate and the shortening of the interval between rasburicase infusions. Conclusions: This is the first report of rasburicase/methotrexate co-treatment in gout. Despite being well tolerated by our patient with D2T tophaceous gout and cardio-renal comorbidities, it did not achieve the expected benefit, with potential development of immunogenicity. More studies are needed to assess the effectiveness and safety of this co-therapy.

Figure 10. Polyarticular chronic tophaceous gout.

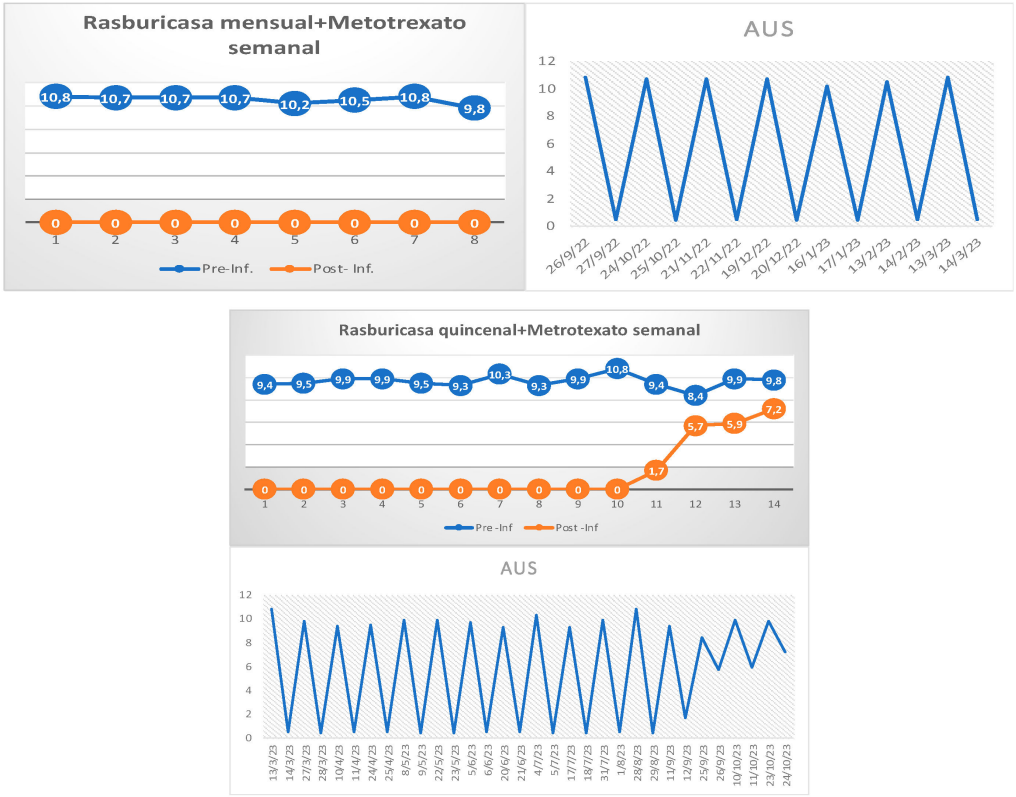

Figure 11. Serum uric acid level fluctuations during treatment with rasburicase/methotrexate co-therapy.

26. Intensive Reduction of Serum Uric Acid through the Uricase Effect through the Combination of Benzbromarone and Febuxostat in Patients with Difficult-to-Treat Tophaceous Gout

Claudia María Gómez-González, Marta Novella-Navarro, Fernando Pérez-Ruiz and Enrique Calvo-Aranda

Rheumatology Resident in Rheumatology Department, Hospital Universitario Infanta Leonor, 28031 Madrid, Spain

Abstract: Background: Some patients with gout have multiple comorbidities and subcutaneous tophi refractory to conventional monotherapy with urate-lowering treatments (ULTs). Uricases may be helpful drugs, but they are not always available. Combined treatment with two potent ULTs, such as FBX and BNZ, could achieve a uricase-like effect and be a therapeutic alternative for these patients. Objective: to evaluate the efficacy and tolerance of the combined treatment of benzbromarone BNZ with FBX in patients with difficult-to-treat (D2T) tophaceous gout. Ours was a multicenter observational study with patients diagnosed with gout according to EULAR/ACR 2015 criteria, subcutaneous tophi, and poor response to standard of care treated with a combination of BNZ and FBX according to a 12-month two-step regimen: FBX monotherapy for the first 6 months (individualized dose optimization) followed by subsequent addition of BNZ (50 mg/day, progressively escalating to 100 mg, whenever possible). Demographic and clinical variables related to gout, cardiovascular risk factors (CVRF), nephrolithiasis, estimated glomerular filtration rate (eGFR), and liver enzymes were collected. A descriptive analysis of the sample was performed using frequencies and percentages for qualitative variables and measures of central tendency and dispersion for quantitative variables. A T-test for paired samples was used to analyze changes in uric acid (UA) levels and eGFR. Results: Fifteen patients were recruited from two hospitals; they were 87% male, with a median age of 59 years (range 43–93), oligo/polyarticular arthritis, and a mean of 5.7 ± 3.7 attacks in the year before starting BNZ. Most of them had advanced gout (mean 16.2 ± 8.8 years) with high

basal UA levels (mean 10.3 ± 1.7 mg/dL), a marked presence of CVRF (93% hypertension, 73% dyslipidemia, 13% major cardiovascular event, 7% diabetes), and renal impairment (mean eGFR 63.7 ± 23.6 mL/min; mean creatinine 1.21 ± 0.37 mg/dL). Only one patient had a history of nephrolithiasis. Before starting combination therapy, 80% had received monotherapy with a xanthine oxidase inhibitor: 27% allopurinol (median 200 mg/day, range 100–300) and 53% FBX (median 100 mg/day, range 40–120). Adding BNZ to FBX treatment resulted in a significant reduction in UA at 12 months (Δ = 2.1 mg/dL [95% CI: 1.2–2.9], $p < 0.001$) in addition to the initial decrease achieved by FBX alone (Δ = 2.3 mg/dL [95% CI: 1.1–3.6], $p = 0.002$; Figure 12), with tophi dissolution in 60% (9/15) of patients. The median duration of follow-up was 18 months (range 9–44); median exposure to BNZ was 12 months (range 6–38). Reasons for discontinuation of BNZ were tophi dissolution in nine patients, loss of follow-up in three patients, and poor clinical tolerance in one patient. There were no serious adverse events, renal colic, or significant changes in liver enzymes or kidney function after 12 months compared to baseline values (eGFR12m 61.6 vs. eGFRbaseline 63.7 mL/min; n.s.). One death was recorded, but it was not treatment-related; the patient was elderly with a history of aortic regurgitation. Conclusions: In our sample, the combination of BNZ and FBX was effective in patients with D2T tophaceous gout, with an intensive reduction in UA and rapid tophi dissolution. Combined therapy was well tolerated by most patients.

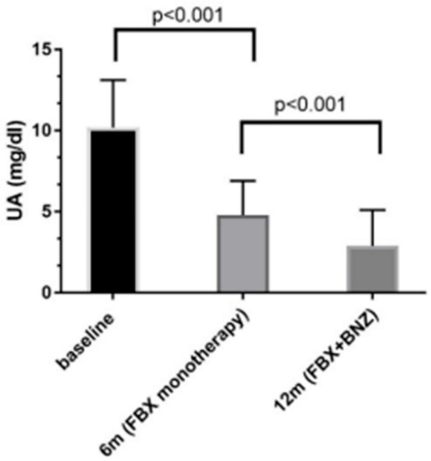

Figure 12. Changes in serum uric acid levels in patients treated with sequential combination therapy. UA: uric acid; FBX: febuxostat; BNZ: benzbromarone.

27. "Gout Was the Boss": A Qualitative Interview Study of Impact of Gout in Work

Cesar Diaz-Torne, Maria A. Pou, Chiara Gasteiger, Anne Horne and Nicola Dalbeth

University of Auckland, Auckland 1010, New Zealand

Abstract: Background: Gout is the most common form of inflammatory arthritis and causes pain, inflammation, and decreased quality of life. Previous qualitative studies have analysed the impact of gout on various domains, but there have been no previous studies designed to examine its impact on employment. Objective: to identify and describe patients' opinions and experiences of the impact of gout on employment. Methodology: Ours was a qualitative study using in-depth, semi-structured face-to-face interviews with persons who had experienced a gout flare during their working years. The study aimed for diverse demographics, job types, and gout characteristics. The interviews were guided by key questions covering impact on employment, job changes, disclosure, and co-worker reactions. Final sample size was determined when the richness, depth, and relevance of the information obtained was adequate and when additional themes were no longer identified. The interviews were collected, recorded, and transcribed in full. Reflective thematic analysis was used for data analysis. Verbatim transcripts of audio recordings were subjected to thematic analysis using NVivo software to facilitate coding, sorting,

and data retrieval. Results: Eighteen participants were included. Demographic, clinical and work characteristics are shown in Table 7. The key themes that emerged from the interviews were grouped into six main categories, as follows. 1. Gout factors: Participants highlighted the intensity of pain, the presence of tophi, and the joints affected as critical factors in understanding how gout impacts employment. Severe flares often made work nearly impossible, while mild flares were considered just an inconvenience. The location of the affected joints also influenced patients' ability to work. 2. Employment factors: Physical requirements and workplace flexibility were significant issues. Jobs with high physical requirements were particularly challenging. Lack of workplace flexibility, including the ability to work remotely, change meeting dates, or adapt tasks, had a significant impact on the patients' ability to continue working. 3. Physical experience: Participants described a wide range of physical experiences, from working with discomfort to being unable to work. Ability to work and concentration were affected by the severity of the flare. Additionally, difficulty in commuting to the workplace was a significant factor. 4. Psychological experience: Patients reported feelings of responsibility, embarrassment, guilt, and depression. Feeling responsible for missed work, reduced efficiency, or the need for help was a common theme. Some felt embarrassed about having gout and tried to hide it, especially younger patients and women. Others experienced guilt, particularly if they believed their disease was self-inflicted. Some patients even reported feeling depressed due to the limitations imposed by gout. 5. Social experience: The effects of gout extended beyond the direct impact of the disease at work and affected other spheres. This included concerns about disclosing the condition at work, the prioritization of work over other life roles, and a negative financial impact. 6. Positive impact of effective gout management: Proper gout management was identified as crucial to improving patient experiences. Understanding the disease, managing acute gout attacks with anti-inflammatories, and adhering to urate-lowering therapy were described as key elements of preventing flares, reducing pain intensity, and maintaining the ability to work. Conclusions: This study sheds light on the multifaceted impact of gout on work and employment, emphasizing the importance of both disease management and workplace adaptations for gout patients.

Table 7. Demographic, clinical, and employment characteristics of the participants.

Participant	Sex	Age (Years)	Gout Duration (Years)	Tophi	Work Roles	Days off Last Year Due to Gout
1	M	62	41	Yes	Wharf worker/Hospitality /Retail	No
2	M	41	8	No	Manager	No
3	M	56	12	No	Architect	No
4	M	54	2	No	Computer programmer	No
5	M	74	14	Yes	Factory maintenance	Retired
6	M	57	3	Yes	Chemist engineer	No
7	M	48	8	No	University teacher	No
8	M	53	9	No	Storeman	Yes
9	M	60	30	Yes	Government officer	Yes
10	M	59	12	No	Engineer/Hospitality	Yes
11	M	49	9	No	Engineer	No
12	M	36	1	No	Project supervisor	Yes
13	F	36	18	Yes	Senior Administrator	Yes
14	F	33	10	No	Service Consultant	Yes
15	M	29	13	Yes	Student/Storeman /Psychologist	Yes
16	M	42	8	No	Secondary school teacher	No
17	M	66	37	No	Factory worker/Commercial	Retired
18	M	67	7	No	Teacher	Retired

28. The Lower Frequency of ST-Elevation Myocardial Infarction in Patients with Gout

Panagiota Drivelegka, Lennart Jacobsson, Tatiana Zverkova-Sandström and Mats Dehlin

Department of Rheumatology and Inflammation Research, Institution of Medicine, Sahlgrenska Academy, University of Gothenburg, 405 30 Göteborg, Sweden

Abstract: Background: Patients with gout are at increased risk of acute myocardial infarction (AMI) [1]. However, its clinical characteristics have not been previously studied. Objectives: The aim of this study was to investigate the clinical characteristics of first-ever AMI in patients with gout compared to the general population. Methodology: Using data from regional and national population-based registers, we identified all patients with a diagnosis of gout at both primary and specialized care in Western Sweden and a first-ever AMI in the period 2006–2016. Each subject was matched on sex and admission year with up to five comparators from the general population. Clinical presentation at admission and clinical course in gout cases and controls were compared by using logistic regression analysis. Results: We identified 1000 patients with gout (men, 72.7%; mean age, 70.0 years) and 4740 matched general population comparators (men, 73.5%; mean age, 71.5 years) with a first-ever AMI. Patients with gout had significantly more comorbidities compared to the general population (Table 8). At admission, patients with gout had significantly lower odds of ST-elevation myocardial infarction (STEMI) (OR, 0.84; 95% CI, 0.72–0.99) and higher odds of atrial fibrillation (AF) (OR, 1.93; 95% CI, 1.62–2.31) and severely depressed left ventricular function (OR, 1.35; 95% CI, 1.00–1.82) (Table 9). Gout patients were significantly more likely to receive treatment with continuous positive airway pressure and less likely to undergo coronary angiography, percutaneous coronary intervention (PCI), or any revascularization during hospitalization (Table 9). The duration of hospitalization for first-ever AMI was longer in gout patients than in controls (7.5 vs. 6.4 days; *p*-value, <0.001). Conclusions: Patients with gout were significantly less likely to present with STEMI at admission for first-ever AMI compared to the general population, but they were more likely to present with AF and severely depressed left ventricular function. Furthermore, they were less likely to undergo coronary angiography and PCI during hospitalization, as compared to the general population.

Table 8. Patient characteristics and comorbidities in gout patients and general population comparators upon admission for a first-ever AMI.

	Gout Cases N = 1000	**Controls § N = 4740**	***p*-Value**	**OR * (95% CI)**
Men, N (%)	727 (72.7)	3485 (73.5)	0.59	
Age, mean (SD), years	70.0 (11.6)	71.5 (11.3)	0.0001	
Comorbidities, N (%)				
CHD	284 (28.4)	978 (20.6)	<0.0001	1.5 (1.3–1.7)
Hypertension	823 (82.3)	2661 (56.1)	<0.0001	3.6 (3.1–4.3)
Diabetes	309 (30.9)	857 (18.1)	<0.0001	2.0 (1.7–2.3)
Obesity	271 (27.1)	793 (16.7)	<0.0001	2.0 (1.7–2.3)
Hyperlipidemia	404 (40.4)	1271 (26.8)	<0.0001	1.9 (1.6–2.1)
Renal disease	225 (22.5)	405 (8.5)	<0.0001	3.1 (2.6–3.7)
Heart failure	207 (20.7)	406 (8.6)	<0.0001	2.7 (2.2–3.3)
Cardiomyopathy	12 (1.2)	24 (0.5)	0.01	2.4 (1.2–4.9)
Atrial fibrillation	212 (21.2)	466 (9.8)	<0.0001	2.4 (2.0–2.9)
Smoking	185 (18.5)	1017 (21.5)	0.04	0.9 (0.7–1.1)
Alcoholism	47 (4.7)	93 (2.0)	<0.0001	2.7 (1.9–3.9)
Cerebrovascular disease	205 (20.5)	598 (12.6)	<0.0001	1.7 (1.4–2.0)
Thromboembolic disease	19 (1.9)	70 (1.5)	0.33	1.2 (0.7–2.1)
Malignancy	95 (9.5)	366 (7.7)	0.06	1.2 (1.0–1.6)
Atherosclerotic disease	113 (11.3)	252 (5.3)	<0.0001	2.2 (1.7–2.7)

Table 8. *Cont.*

	Gout Cases N = 1000	Controls § N = 4740	*p*-Value	OR * (95% CI)
Co-medication, N (%)				
CVD drugs ¤	733 (73.3)	2323 (49.0)	<0.0001	2.9 (2.5–3.3)
Anticoagulants/ Antiplatelet drugs	462 (46.2)	1408 (29.7)	<0.0001	2.0 (1.7–2.3)
Allopurinol	350 (35.0)	32 (0.7)	<0.0001	78.5 (54.2–113.8)
Colchicine	3 (0.3)	5 (0.1)	0.13	3.2 (0.8–13.3)
Cortisone	149 (14.9)	259 (5.5)	<0.0001	2.9 (2.4–3.7)

§ Matched on sex and admission year. * Adjusted for age. ¤ Vasodilator drugs, anti-hypertensive drugs, diuretics, beta-blockers, calcium antagonists, and renin–angiotensin–aldosterone inhibitors. AMI, acute myocardial infarction; CHD, coronary heart disease; CVD, cardiovascular; OR, odds ratio; CI, confidence interval.

Table 9. Characteristics of the first-ever AMI in gout patients compared to controls from the general population §.

Characteristics	Gout Cases N = 1000	Controls N = 4740	OR * (95% CI)
Clinical presentation			
ST-elevation	246 (24.6)	1333 (28.1)	0.84 (0.72–0.99)
Non-ST-elevation	481 (48.1)	2150 (45.4)	1.09 (0.95–1.25)
Cardiogenic chock	25 (2.5)	101 (2.1)	1.16 (0.74–1.81)
Atrial fibrillation	221 (22.1)	585 (12.3)	1.93 (1.62–2.31)
AV block	17 (1.7)	102 (2.2)	0.75 (0.44–1.25)
Left ventricular function			
Normal (≥50%)	547 (54.7)	2688 (56.7)	reference
Slightly depressed (40–49%)	148 (14.8)	722 (16.3)	0.92 (0.75–1.12)
Moderately depressed (30–39%)	82 (8.2)	381 (8.0)	1.01 (0.78–1.31)
Severely depressed (<30%)	62 (6.2)	211 (4.5)	1.35 (1.00–1.82)
In-hospital course			
Coronary angiography	726 (72.6)	3734 (78.8)	0.77 (0.65–0.92)
Any primary reperfusion	238 (23.8)	1459 (30.8)	0.73 (0.62–0.86)
PCI	231 (23.1)	1408 (29.7)	0.74 (0.63–0.87)
Acute CABG	3 (0.3)	13 (0.3)	1.15 (0.33–4.03)
CPAP	69 (6.9)	190 (4.0)	1.70 (1.28–2.26)
PM/ICD	19 (1.9)	53 (1.1)	1.65 (0.97–2.79)

Reference

1. Drivelegka, P.; Jacobsson, L.T.H.; Lindsrtom, U.; Bengtsson, K.; Dehlin, M. Incident Gout and Risk of First-Time Acute Coronary Syndrome: A Prospective, Population-Based Cohort Study in Sweden. *Arthritis Care Res.* **2023**, *75*, 1292–1299.

29. Developing a Pharmacological Trial in CPPD: Towards the Conquest of Ithaca!

Georgios Filippou [1,2], Silvia Sirotti [1], Carlo Scirè [3] and Lene Terslev [4]

1 Rheumatology Unit, IRCCS Ospedale Galeazzi, Sant'Ambrogio, 20157 Milan, Italy
2 Department of Biomedical and Clinical Sciences, University of Milan, 20122 Milan, Italy
3 School of Medicine and Surgery, University of Milano-Bicocca, 20126 Milan, Italy
4 Center for Rheumatology and Spine Diseases, Rigshospitalet, 2100 Copenhagen, Denmark

Abstract: Background: Calcium pyrophosphate deposition (CPPD) is a prevalent condition, particularly among the elderly. Individuals affected by CPPD may develop arthritis, which can affect a single joint or multiple joints, including small, large, and/or axial joints. However, there is currently no specific treatment for this condition, and patients are often

managed using off-label drugs to alleviate symptoms. The absence of experimental or animal models represents a significant hurdle in the development and testing of novel drugs, contributing to a comparatively slow pace of research in this domain, especially when contrasted with advancements in other rheumatic diseases. Consequently, clinical pharmacological trials emerge as the only alternative for evaluating potential treatments in CPPD disease. Objective: This abstract outlines the challenges encountered and overcome during the initiation of a pharmacological trial for CPPD disease. Methodology and Results: In 2023, the IRCCS Galeazzi–Sant'Ambrogio Hospital successfully secured funding from Eli Lilly for a pivotal pharmacological trial investigating the efficacy of baricitinib in treating CPPD disease. Given the unclear pathogenesis of crystal deposition and the absence of known deposition-reducing drugs, a promising treatment for CPPD disease should focus on reducing inflammation, subsequently alleviating pain, and minimizing joint damage. According to available data on the pathogenesis of arthritis in CPPD, baricitininb appears to be promising in reducing inflammation, as it interacts with the pathways of some of the most overexpressed cytokines in CPPD disease. The efforts leading to the agreement for this pharmacological trial commenced in 2018, taking five years to finalize. Despite facing setbacks due to the pandemic, various obstacles, both bureaucratic (such as new European trial regulations and intellectual property issues) and scientific (classification criteria for CPPD disease, which were developed after the submission of the protocol; patient classification based on disease phenotype; defining outcomes; determining the standard of care; and justifying off-label use of drugs for the control group, etc.), had to be addressed. Finally, according to the new European regulation, a Contract Research Organization (CRO) had to be engaged in order to guarantee data quality and submission of the trial in the relevant organisms for approval, with a remarkable impact on the total budget of the trial. Despite addressing all the challenges diligently with the best scientific and legal knowledge available, the potential for substantial modifications to the protocol by the ethics committee remains a major concern. Conclusions: Although CPPD is a prevalent condition, it remains largely neglected. Limited awareness within the scientific community and the general population contributes to CPPD being both underdiagnosed and underestimated. This inevitably impacts the development of clinical trial protocols, both formally and scientifically. Successful collaboration among different stakeholders (scientific, administrative, and legal) is crucial to overcoming the challenges encountered during the development of pharmacological trials for CPPD disease. All the challenges outlined form a comprehensive research agenda on CPPD, requiring resolution to facilitate quicker and more effective development of clinical trials for this condition.

30. Improved Diagnostic Performance in the Detection and Characterization of Crystals Related to Arthropathies with Photon-Counting Detector Computed Tomography

Florian A. Huber [1,*], David Rotzinger [2], Matthias Zadory [3], Felix C. Müller [4], Anna Døssing [5], Veronique Schuppli [1], Lukas Moser [1], John M. Froehlich [3], Hatem Alkadhi [1] and Fabio Becce [2]

1 Institute of Diagnostic and Interventional Radiology, University Hospital Zurich and Faculty of Medicine, University of Zurich, 8006 Zurich, Switzerland
2 Department of Diagnostic and Interventional Radiology, Lausanne University Hospital and University of Lausanne, 1005 Lausanne, Switzerland
3 KlusLab Research, 8032 Zurich, Switzerland
4 Department of Radiology, Herlev and Gentofte Hospital, University of Copenhagen, 1172 Copenhagen, Denmark
5 The Parker Institute, Bispebjerg and Frederiksberg Hospital, 2000 Frederiksberg, Denmark
* Correspondence: florian.huber@usz.ch

Abstract: Our objective was to assess the diagnostic performance of the first ever clinical photon-counting detector (PCD) computed tomography (CT) scanner with regard to the detection and differentiation of calcium hydroxyapatite (HA) vs. calcium pyrophosphate

(CPP) and to compare it with routine energy-integrating detector (EID)-CT. We performed a prospective in vitro phantom study. Therefore, we used custom-made industry-standard cylindric rods of CPP and HA (both 50, 100, 200 mg/mL). We scanned all samples with PCD-CT twice (at 120 kV and 140 kV) and with the standard-of-care EID-CT (dual-source scanner at 80 kV and tin-filtered (Sn) 150 kV). All scans were performed with an identical and clinically realistic dose using a CT dose index of 8 milligray. Ten fixed-size region-of-interest measurements of 50 voxels each were performed on axial reconstructions per rod and series, respectively. We calculated dual-energy (DE) CT ratios for each material in each scanner. ROC curves and respective AUC values with 95% confidence intervals were calculated to assess differentiability of CPP vs. HA for each scan setting. In addition, we assessed the limit of detection (LOD, in mg/mL) for both materials (per 50-voxel ROI and per voxel, separately) using linear regression coefficients of attenuation as a function of concentration. DECT ratios were slightly different between CPP and HA in EID-CT and in PCD-CT scans. AUC values for the performance of differentiation between CPP and HA were significantly higher in PCD-CT scans (AUC: 0.969 and 0.987 vs. 0.874 for PCD-CT at 120 kV and 140 kV vs. EID-CT; $p < 0.05$). The LOD was overall comparable between methods, with the lowest LOD for CPP ranging from 7.69 to 10.84 mg/mL per voxel and from 2.61 to 3.45 mg/mL per ROI, compared to 8.18–9.98 mg/mL per voxel and 2.44–3.51 mg/mL per ROI for HA across the different scan methods. In conclusion, we provide preclinical proof of principle that the detection and characterization of calcium-based crystals can be performed with PCD-CT, showing improved performance compared to the best-performing EID-CT, with excellent accuracy. These first results are promising with respect to the potential development of a reliable imaging assessment method for the differentiation and characterization of calcium-based crystal load involved in symptomatic arthropathies. Further studies will be required to demonstrate comparable diagnostic confidence in PCD-CT in clinical settings.

Funding: This research received no external funding.

Conflicts of Interest: Unrestricted fundings from AMGEN Rare disease/Horizon Pharmaceuticals, OLATEC, SOBI.

Reference

1. Lioté, F.; Perez-Ruiz, F.; Ea, H.-K.; Merriman, T.; Pascart, T.; So, A. 14th European Crystal Network (ECN) Workshop—Abstract Proceedings. *Gout Urate Cryst. Depos. Dis.* **2024**, *2*, 60–69. [CrossRef]